Phytoplankton Production and Biomass in Arctic and Sub-Arctic Marine Waters During the Summers of 2007 and 2008

by

Ian A. Wrohan
Bachelor of Science, University of Victoria, 2005

A Thesis Submitted in Partial Fulfillment
of the Requirements for the Degree of

MASTER OF SCIENCE

in the School of Earth and Ocean Sciences

Supervisory Committee

Phytoplankton Production and Biomass in Arctic and Sub-Arctic Marine Waters During the Summers of 2007 and 2008

by

Ian A. Wrohan
Bachelor of Science, University of Victoria, 2005

Supervisory Committee

Dr. Diana E. Varela, Department of Biology/School of Earth and Ocean Sciences
Supervisor

Dr. S. Kim Juniper, Department of Biology
Departmental Member

Dr. Roberta C. Hamme, School of Earth and Ocean Sciences
Departmental Member

Abstract

Supervisory Committee
Dr. Diana E. Varela, Department of Biology/School of Earth and Ocean Sciences
Supervisor
Dr. S. Kim Juniper, Department of Biology
Departmental Member
Dr. Roberta C. Hamme, School of Earth and Ocean Sciences
Departmental Member

During the summers of 2007 and 2008, we determined net, new and regenerated primary production and phytoplankton biomass in Arctic and Sub-Arctic marine waters around North America. Carbon and nitrogen uptake rates were measured using the ^{15}N and ^{13}C tracer technique in 24-hr on-deck incubations, and phytoplankton biomass was determined by *in vitro* fluorometry. Average net primary production was highest in the north Bering and south Chukchi Seas (998 mg C m^{-2} d^{-1}) and defined as primarily new production (f-ratio of 0.57), potentially indicating high particulate export from surface waters. Phytoplankton biomass was also high (39 mg chl *a* m^{-2}) in this region and comprised mostly (61%) of cells >5 μm, supporting the conclusion of a high export system. Average net primary production was lowest in the Canada Basin (50 mg C m^{-2} d^{-1}) with an f-ratio of 0.17 and characterized by low phytoplankton biomass (8 mg chl *a* m^{-2}), comprised of mostly (19%) cells <5 μm. In much of the study area, the presence of ice cover appeared influential in affecting Arctic primary production patterns. Water column stratification in the wake of retreating sea ice produced conditions favorable to initiating seasonal blooms, which most likely terminated due to nutrient exhaustion. Areas characterized by persistent sea ice cover were particularly unproductive, most likely due to light limitation, and nutrient exhaustion due to reduced wind-mixing. These results indicate that primary production in Arctic and Sub-Arctic waters is highly variable, and

provide an important baseline for future studies of phytoplankton dynamics in this rapidly changing region.

Table of Contents

List of Tables

List of Figures

Acknowledgments

I would like to give my sincere thanks to all of those who have helped me in producing this thesis, and name just a few here. To Dr. Eddy Carmack, without who's vision this project would never have come to be. To all those at the Institute of Ocean Sciences, who it's been my pleasure to work with and learn from. To my lab mates, who put up with my bad housekeeping and always had a sympathetic ear. To the faculty and staff of UVic for answering all of my often inane questions. To the crew of the CCGS Louis S. St. Laurent and Sir Wilfrid Laurier for never saying no to just one more rosette cast. To Dave and the staff of the UVic machine shop, from who I learned that oceanography is half scientific investigation, and half plumbing. To the SEOS office staff for their patience as I signed every time-sensitive form typically several hours late. To my supervisory committee, Drs. Kim Juniper and Roberta Hamme, for their attention to detail and guidance along the way. And to my supervisor, Dr. Diana Varela, goes my deepest thanks and appreciation; without her compassion, patience, and subtle guidance I might have floated away from this incredible project long ago.

CHAPTER 1. INTRODUCTION

1.1. The Oceanographic Role of Phytoplankton

1.1.1. Phytoplankton Metabolism and Nutrient Cycling

During cellular metabolism, phytoplankton acquire and release carbon (C), nitrogen (N), phosphorus (P) and, in the case of siliceous forms, silicon (Si), and are thus instrumental in regulating the cycling of these elements in the marine environment (Syrett, 1981). At normal ocean acidity (pH of 8.1 to 8.3) carbon exists, for the most part, as bicarbonate ion (HCO_3^-), the main source of C available for phytoplankton metabolism (Reynolds, 2006). Nitrogen appears in several dissolved forms, including nitrate (NO_3^-), ammonium (NH_4^+), and urea ($(NH_3)_2CO$). In addition to regulating the pools of these dissolved nutrients, phytoplankton production accounts for 25% of global primary production (Field et al., 1998), and has a significant effect on atmospheric C via a phenomenon known as the biological pump.

1.1.2. The Biological Pump

The biological pump can be defined as the biologically-mediated transport of organic carbon from the euphotic zone to the deep ocean (Eppley & Peterson, 1979). If one assumes that C fixation is carried out by phytoplankton and that a portion of the dissolved inorganic carbon (DIC) in the euphotic zone is from the atmosphere, then a C pathway can be identified. Atmospheric carbon dioxide dissolves into surface waters where it is taken up by phytoplankton during photosynthesis. This biologically fixed C can sink into deeper water upon phytoplankton death and/or vertical transport in fecal pellets or marine snow, thereby forming a mechanism by which C moves from the

atmosphere to the deep ocean. The ultimate fate of the fixed C can be assessed by breaking up the primary production that occurs in the euphotic zone into its new and regenerated forms, as described below.

1.1.3. Net, New and Regenerated Primary Production

Aquatic primary production is defined here as the production of organic compounds (e.g. sugars) from dissolved inorganic carbon through the process of photosynthesis. In this thesis, the term 'net primary production' (NPP) will be used to represent the total amount of particulate organic carbon fixed by phytoplankton that remains after losses from cellular respiration.

Organic material leaving the euphotic zone must be replaced with external inputs to maintain steady-state. The portion of total primary production based on N forms (primarily NO_3^-) from external sources is referred to as new production, while that based on N recycled within the euphotic zone (such as NH_4^+ and urea) is known as regenerated production (Dugdale & Goering, 1967). In the open ocean, NO_3^- that fuels new production is thought to come primarily from upwelling and vertical mixing from deep waters, having been remineralized below the euphotic zone from N exported from within the euphotic zone (Eppley & Peterson, 1979). While this may certainly be true in the open ocean, in coastal waters the origin of the N which drives new production is typically a much more complex issue because terrestrial inputs and horizontal advection must also be taken into account.

New production is generally reported on a percent basis (% of net primary production) or as an 'f-ratio' (Dugdale & Goering, 1967). Though the interpretation of the f-ratio is at times controversial (Ward, 1986), the calculation itself is simply the ratio

of new production to total (new plus regenerated) production. Thus, a high ratio suggests a high proportion of new production, which is often characterized by larger cells, and tends to be indicative of high C export to deeper waters, and efficient transfer of energy to higher trophic levels (Eppley & Peterson, 1979). Determining the magnitude of new and regenerated production is thus critical for understanding the role of phytoplankton in C and N cycling.

In nutrient-rich areas, diatoms and other large cells are typically present and are rapidly exported, accounting for over 50% of NPP (an f-ratio of >0.5). In oligotrophic areas, export can be as low as 5 to 10% of NPP (Falkowski & Raven, 2007). Smaller cells appear to contribute more to the regenerated cycle due to their low sinking rates (Grebmeier & Barry, 1991).

1.1.4. Environmental Factors Affecting Primary Production

The growth of autotrophic cells is limited by the availability of an adequate supply of both nutrients and photosynthetically active radiation (PAR) to drive photosynthesis. Inputs from terrestrial sources, such as rainwater runoff, riverine discharges and aeolian dust can supply nutrients to the marine environment, enhancing or limiting phytoplankton production. At the continental shelf margins, upwelling of nutrients from deeper waters can also plays a significant role in supplying nutrients to surface waters.

The availability of solar radiation in the polar latitudes is influenced by seasonality and ice cover. Incoming solar irradiance in the Northern hemisphere is dramatically reduced or negligible during the winter months, almost completely limiting photosynthesis (Arrigo et al., 2008; Gosselin et al., 1997), and sea ice cover reduces

primary production markedly by screening PAR, often preventing phytoplankton blooms from initiating (Arrigo & van Dijken, 2004). Persistent sea ice also insulates the upper water column from the atmosphere, thereby reducing or eliminating wind-driven mixing, preventing water from moving away from shore and thus limiting coastal upwelling events (Carmack & Chapman, 2003), thereby reducing nutrient inputs from deeper waters.

The freeze-thaw cycle can affect phytoplankton production differently, depending on the season. Melting sea ice (in the spring) can promote ice edge blooms in the wake of the retreating summer icepack by temporarily increasing upper ocean stability as a result of fresh water being released into the upper water column during ice retreat (Lancelot et al., 1993; Legendre et al., 1992; Schandelmeier & Alexander, 1981; Smith et al., 1987). A re-freezing ice pack (in the autumn) can lead to brine rejection, and thus instability in the water column resulting in vertical mixing (Mathews, 1981; Smith et al., 1985). This effect, in the presence of light sea ice cover and increased wind mixing, can be instrumental in initiating autumn phytoplankton blooms.

1.2. Physical Oceanography of Arctic and Sub-Arctic Oceans

The physical oceanographic structure of the Arctic Basin results from inputs of ocean water from the Pacific and Atlantic Oceans, inputs from several major river plumes, and the seasonal ice cycle. Atlantic water enters the Arctic basin by way of the Barents Sea, off the Norwegian coast, and into Baffin Bay via the West Greenland Current (Fig. 1.1). Atlantic inflow into the Arctic basin is five times higher than that of the Pacific Ocean (Woodgate et al., 2005). Pacific water enters the Arctic basin from the Bering Sea via the Bering Strait, due to a height difference of 0.5m on the Bering Sea side (Stabeno et al.,

2006). The origin of much of the Pacific water is the North Pacific Current, which bifurcates off the North American coast, moving northwards as the Alaska Current and

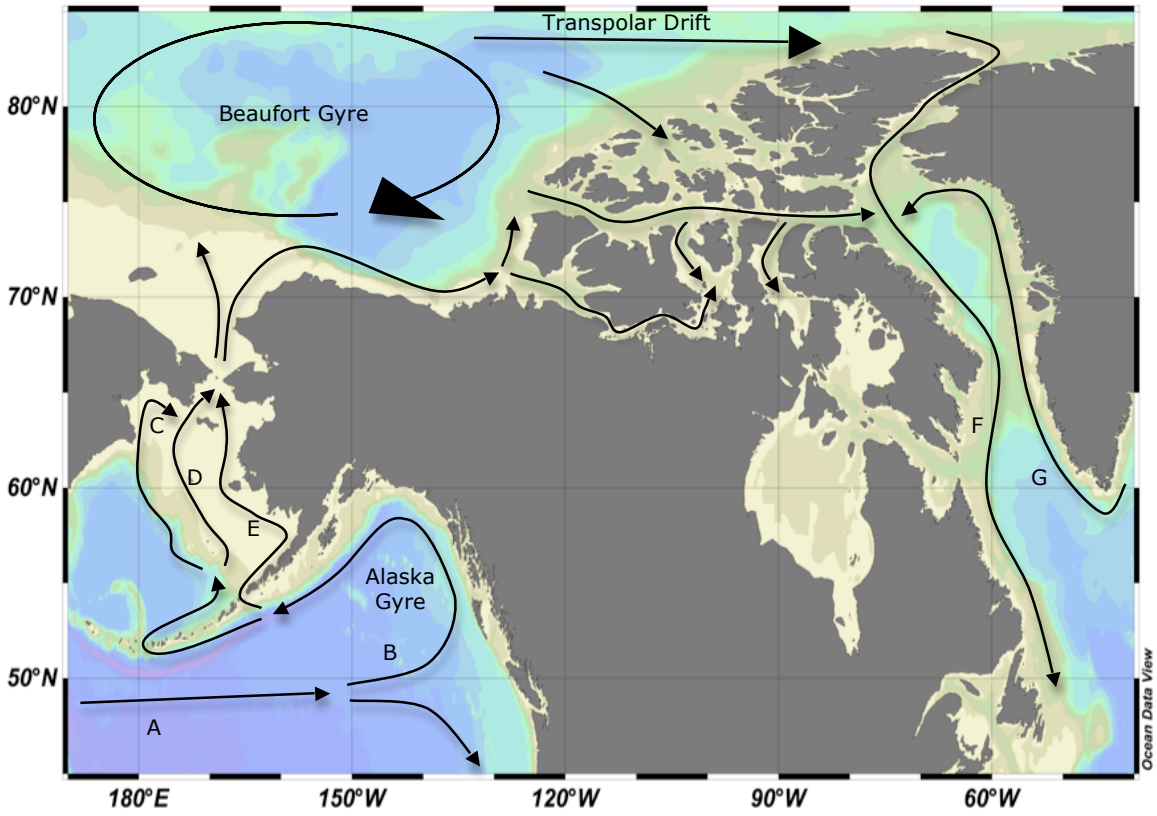

Figure 1.1. Ocean currents for the regions discussed in this thesis. A. North Pacific Current; B. Alaska Current; C. Anadyr Water; D. Bering Shelf Water; E. Alaska Coastal Water; F. Baffin Current; G. West Greenland Current. (adapted from Carmack & Wassman, 2006; Kostianoy et al., 2004).

forming the Alaska Gyre. Upon reaching the Aleutian Islands this water moves northwards through the islands in several locations, ultimately resulting in the formation of the distinct currents: the Alaska Coastal Water, the Bering Shelf Water, and the northern branch of the Anadyr Current, which all converge in the northern Bering Sea and pass through the Bering Strait (Woodgate et al., 2005). In the Canada Basin, Pacific water is present in a layer from 40 to 200 m under the mixed layer and on top of

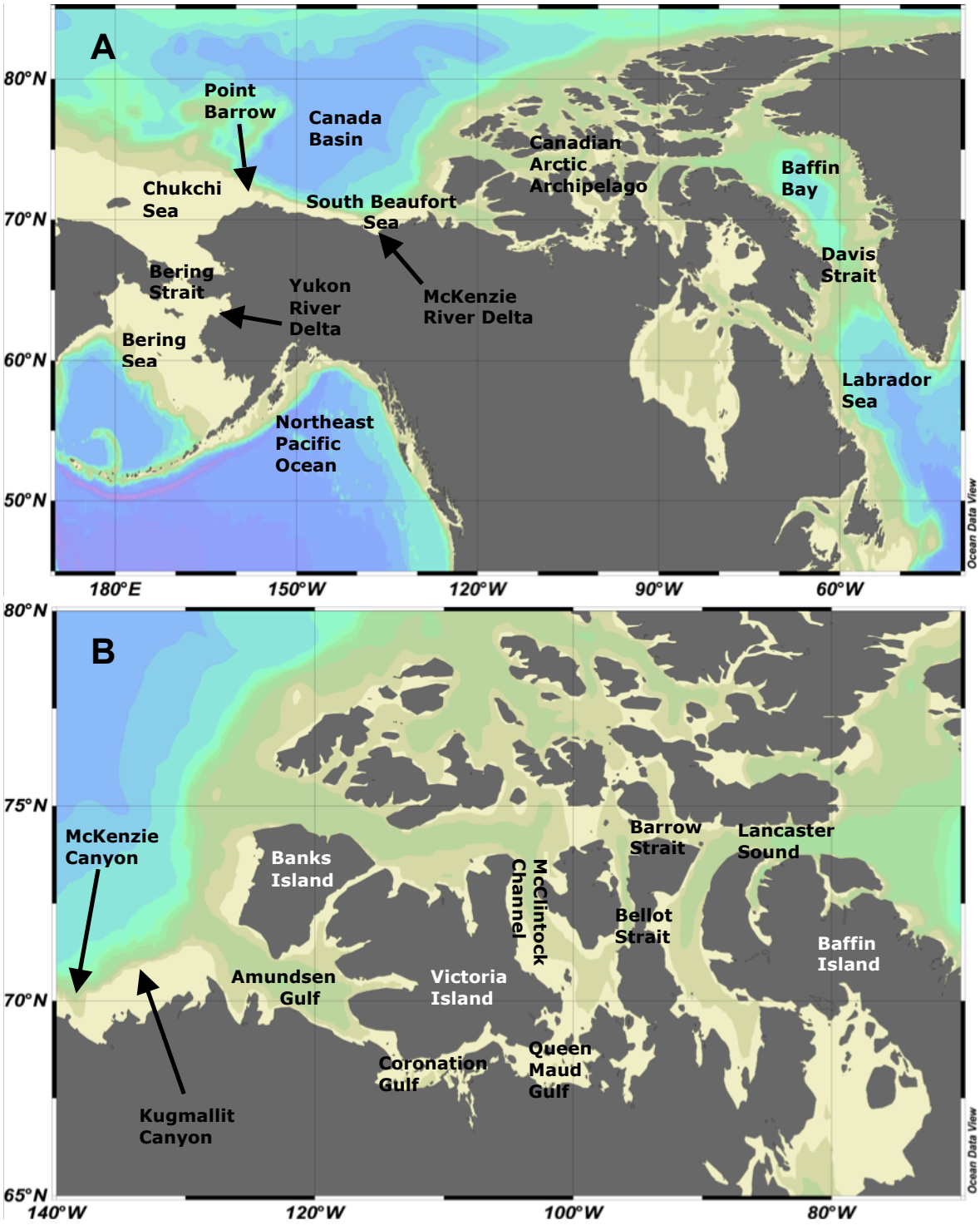

Figure 1.2. A: Locations of geographic areas in Arctic and Sub-Arctic Oceans sampled during the C3O project in the summers of 2007 and 2008, and mentioned in this thesis. B: This lower map shows in more detail locations in the Canadian Arctic Archipelago and McKenzie River Delta.

Atlantic-origin water, exiting through Fram Strait (east of Greenland) and the Canadian Arctic Archipelago (Carmack & Wassman, 2006; Jones et al., 2003).

The dominant surface current in the Arctic Basin forms the Beaufort Gyre, which moves in a clockwise rotation and forces surface water through the Canadian Arctic Archipelago (Fig. 1.1 and 1.2A). The wind-driven transpolar drift carries water and ice towards the northern tip of Greenland. Atlantic water enters Baffin Bay from the north via Nares Strait, or from the South after moving around the southern tip of Greenland via the West Greenland Current. The strength of the Beaufort Gyre, which typically dictates the overall movement of water in the Arctic basin, was greater in 2008 than in 2007 (Woods Hole Oceanographic Institution, 2010). A deeper current, the Beaufort Undercurrent, flows in the opposite direction (counter-clockwise), moving water eastwards along the continental margin and playing a role in coastal upwelling in the Beaufort Shelf and Chukchi Sea, but having very little effect on surface water movement (MacDonald et al., 1989). The net flow of water through the Canadian Arctic Archipelago is eastward, from the Arctic Ocean to Baffin Bay and Labrador Sea, due to the difference in sea level (Walker, 1977).

1.3. The Shelf-Type Regional Classification Scheme

The Arctic/Sub-Arctic region is a far too geographically vast an area to permit making broad generalizations about the physical and chemical controls on biological activity. It is therefore helpful to subdivide the study area into discrete geographic regions prior to analysis. But what criteria are appropriate for this subdivision? Solar radiation and nutrient supply were mentioned in Chapter 1 as the two most important factors regulating primary production and deserve mention. Solar radiation is the somewhat more

consistent and predictable of these two factors, as the nutrient supply is determined not only by in situ processes, such as excretion and local terrestrial inputs, but also by the influx of nutrients via upwelling or advection from adjacent water masses. As such, continental shelves - especially continental shelf breaks - are biologically important areas due to the role that topography plays in oceanic mixing process. The shallow waters overlaying continental shelves make up over 50% of the surface area of the Arctic marine waters and are responsible for 84% of high Arctic primary production (Carmack, 2004; Michel et al., 2006).

Carmack & Wassmann (2006) surmised that a physics-driven approach to dividing the study area up into discrete regions is appropriate given the bottom-up control of water properties and movements on the associated biological activity. They identify shelf ecosystems as the most biologically dynamic areas in the ocean, and define them as 'inflow', 'interior', and 'outflow' shelves. Inflow shelves are those who are under the influence of water entering the Arctic basin, interior shelves are the site of transiting water, and outflow shelves are influenced by the egress of water into other ocean basins (as per Carmack & Wassman, 2006) A fourth category is 'basins', which are characterized by the lack of shelf topology; they are typically very deep and lack the shallow-water physical processes that are present in shelf regions.

This regional approach is a way of dividing the large study area covered in this thesis into smaller geographic regions. In this way, regional inferences about phytoplankton production can be more accurately related to the distinct physical and biological properties of the area.

1.4. Primary Production and Phytoplankton Biomass in Arctic and Sub-Arctic Marine Waters

For the purposes of introducing the biological aspects of the vast geographic region covered in this thesis, the aforementioned regional perspective will be used, discussing the areas labelled in Fig. 1.2A. This approach will be used in order to compare spatial patterns of primary production, with the ultimate aim of identifying trends that can be attributed to the underlying physical processes. The following review draws on the work of a number of different authors, using a multitude of methods to produce a summary of primary production over the last several decades.

1.4.1. Northeast Pacific Ocean

For the purposes of this project the northeast Pacific Ocean encompasses the waters constrained by the west coast of North America and the Aleutian Island chain. Most of the northeast Pacific can be considered a basin, except for the coastal regions that have shelf topography. Although replete with nitrate, phytoplankton biomass in the central basin is limited primarily by the availability of iron (Boyd et al., 2004; Tsuda et al., 2003; Martin & Fitzwater, 1988), carried into this HNLC region by aeolian dust (Gao et al., 2001). Typical net primary production (NPP) in the basin ranges from 300 to 600 mg C m^{-2} d^{-1} (Harrison et al., 1999) with an average f-ratio of 0.32 (Peña & Varela, 2007), indicative of a region of low particulate export to deep waters.

In contrast to the oceanic basin, the coastal area off of Vancouver Island has NPP values of >3000 mg C m^{-2} d^{-1} (Boyd & Harrison, 1999), governed by the local macronutrient supply. Primary production on the eastern side of the Aleutian Islands is extremely variable, ranging from 220 to 3810 mg C m^{-2} d^{-1} (Mordy et al., 2005). This

variability is a result of the presence or absence of sporadic upwelling events, dictating whether the current nutrient regime is primarily influenced by the nutrient-poor nearshore waters of the Alaska Current, or nutrient-rich deeper waters (McRoy et al., 1972; Mordy et al., 2005).

1.4.2. Bering and Chukchi Seas

The Bering Sea is defined here as the area north of the Aleutian Island chain and south of the Bering Strait, with all stations visited in this study lying east of 174°W. The Chukchi Sea lies north of strait, with its eastern boundary ending in the vicinity of Point Barrow and all stations lying east of 169°W (Fig. 1.2A; Table A1).

In the Bering Sea, primary production can be as high as 16,000 mg C m^{-2} d^{-1} with an associated f-ratio of 0.8, but on average lower, it is around 500 mg C m^{-2} d^{-1} with f-ratios ranging from 0.1 to 0.5 (Springer & McRoy, 1993; Walsh et al., 1989). The Yukon River injects nutrients into the northeastern Bering Sea, supplying enough fresh water through the Bering Strait to cause significant stratification and stabilization of the upper water column. This results in a phytoplankton spring bloom that moves north with the retreating sea ice that is dominated by diatoms, due to sufficient or elevated $Si(OH)_4$ concentrations and lack of grazing pressure (Wilkinson et al., 2009).

Primary production in the southern Chukchi Sea is fueled by the nutrient-rich waters which flow north through the Bering Strait (Carmack et al., 2006), and Springer & McRoy (1993) found some of the highest primary production rates in the Arctic just north of the strait (~15,000 mg C m^{-2} d^{-1}). Although chlorophyll biomass is greatly reduced under the characteristic winter ice cover in the Chukchi Sea, this region experiences intense blooms which follow the seasonal ice retreat (Wang et al., 2005).

During the summer months primary production in the central Chukchi Sea is variable. Bates et al. (2005) and Cota et al. (1996) measured an average net primary production on the mid-shelf of the Chukchi Sea of 340 and 336 mg C m^{-2} d^{-1} during the summer months, respectively, while Hansell et al. (1993) reported production rates as high as 6000 mg C m^{-2} d^{-1}.

The nutrient-replete water of the Alaska Coastal Current follows the Alaska coast, fueling productivity in the eastern Chukchi, and by the time it arrives at Point Barrow, has lost most of its nutrient load (Hill & Cota, 2005). At this point, most of the current exits through the Barrow Canyon (157^{o}W, 71.5^{o}N), joining a sub-surface current that flows eastward along the shelf break, below the euphotic zone, although some water is thought to round Point Barrow and stay close to the coast (Aagaard, 1984). The Barrow Canyon itself is the site of periodic upwelling from the deeper waters of the Canada Basin, leading to sporadic bloom events resulting in high production such as the 8000 mg C m^{-2} d^{-1} (Hill & Cota, 2005).The continental margin marks the border between the Chukchi Sea and Canada Basin. Along the shelf break, primary production is typically lower than that found in the central Chukchi and heavily influenced by sporadic upwelling events. Hill & Cota (2005) reported a wide range of primary production values (80 to 2900 mg C m^{-2} d^{-1}) along the shelf break between July and August, while Gosselin et al. (1997), found NPP to be 48 mg C m^{-2} d^{-1} on the upper continental shelfbreak. Therefore, primary production on the Chukchi shelf break reaches similar levels to those highly productive coastal upwelling zones (Lalli & Parsons, 1995).

1.4.3. South Beaufort Sea

What will be referred to as the South Beaufort Sea in this thesis are the waters overlaying the continental shelf and slope (to a depth 1000 m), the extent of which is commonly demarked by a line stretching from Point Barrow to slightly north of Banks Island (Figs. 1.2A and 1.2B). The western portion of the shelf, adjacent to the Chukchi Sea, is relatively unproductive due to its shallow depth dominated by riverine runoff, creating low salinity and high turbidity (Sakshaug, 2004).

The physical properties of the McKenzie River delta are governed by both riverine inputs and the influence of oceanic water. In that region, the shelf is ~530 km wide, reaching ~120 km towards the deeper waters of the Canada basin, and is approximately 80 m deep at its furthest northern extent. The depth at which the shelf break occurs creates a condition in which any water upwelled into the area is mostly of nutrient-rich Pacific origin. The magnitude of the upwelling is potentially increased by the presence of the submarine McKenzie (~138^{o}W) and Kugmallit (~134^{o}W) Canyons that border the shelf (Carmack et al., 2004). The McKenzie River inputs typically make up the upper 5 to 10 m of the water column, dominating surface water properties, especially in the summer when runoff is highest (Carmack et al., 2004; Omstedt et al., 1994).

The Beaufort Undercurrent may also inject nutrient-laden Atlantic water onto the shelf through occasional wind-driven upwelling events, but the majority of the shelf-water, especially in the summer, is derived from Pacific water (Aagaard et al. 1989).

1.4.4. Canada Basin

The Canada Basin is the deep water constrained by the Chukchi Sea to the west, Beaufort Shelf to the south, and Canadian Arctic Archipelago to the east. Defined by its lack of continental shelf area, the basin is ~3600 m at its deepest point, and characterized by the presence of both seasonal and multiyear ice pack (Carmack & Wassman, 2006). In this basin, a layer of primarily Pacific-origin water, being both fresh and warm, sits on top of Atlantic-origin water (McLaughlin et al., 2004a; Michel et al., 2006). Primary production throughout the Canada Basin is low, especially when local ice cover is heavy (Hsaio,1977; McRoy, 1993). South of 75°N, Cota et al. (1996) reported primary production rates ranging from 47 to 120 mg C m^{-2} d^{-1}, while Lee & Whitledge (2005) estimated NPP of 106 mg C m^{-2} d^{-1} in the central basin, possibly due to heavy zooplankton grazing (Carmack & Wassman, 2006).

1.4.5. Canadian Arctic Archipelago

The CAA refers to the group of islands and interspersed waterways to the north of the mainland Arctic coast of North America, between the Canada Basin to the west, and Baffin Bay to the east. Although the CAA makes up almost a quarter of the shelf region in the Arctic Ocean, this thesis focuses only on the portion south of 75^{o}N.
Carmack & Wassman (2006) describe the CAA as an "complex network of channels, sub-basins and sills", which connects the Arctic Ocean to the Atlantic Ocean across a vast continental shelf (Fig. 1.2B). Water transiting the CAA has highly variable residence times, and thus significant time for biogeochemical modification (McLaughlin et al., 2004b). This dynamic hydrology, aided by high seasonal stratification due to freshwater inputs from rivers, glacial runoff, and seasonal sea ice melt, creates a biologically

dynamic environment supporting up to 32% of all Arctic shelf primary production (Carmack & Wassman, 2006; Michel et al., 2006; Spence & Burke, 2008).

Dispersed throughout the Arctic marine system are 'polynyas', isolated ice-free areas formed by vertical mixing of deeper, nutrient-rich water which have the potential to substantially increase the productivity of an area that would otherwise be less productive (Michel et al., 2006). Two prominent polynyas exist in the CAA that are relevant to this study: at the eastern end of Bellot Strait and in Lancaster Sound.

Primary production estimates for the CAA are few and, as is the case with NPP estimates, they are seasonally variable. Welch & Kalff (1975) reported summer values of 375 mg C m^{-2} d^{-1} in the vicinity of Resolute Bay, while Brugel et al. (2009) estimated 75 mg C m^{-2} d^{-1} in Amundsen Gulf, but during the early autumn.

1.4.6. Baffin Bay and Davis Strait

Baffin Bay is the basin that lies between the CAA and the west coast of Greenland, and reaches 2136 m at its deepest point. Davis Strait is the relatively shallow body of water (<2000 m) that separates Baffin Bay from the Labrador Sea to the south. Baffin Bay is under the influence of two distinct currents: the Baffin Current on the west side of the bay, along the Baffin Island coast, and the West Greenland Current on the east side of the bay, along the west coast of Greenland (Jensen et al., 1999).

In addition to the presence of land-fast ice along both coasts, Baffin Bay is seasonally ice-covered, which can play a role in creating variable primary production rates. The coasts of Greenland and Baffin Island are cited as the most productive areas in this region due to the many enclosed fjords and glacier-fed inlets where primary production can be over 800 mg C m^{-2} d^{-1} (Dunbar, 1982; Andersen, 1981). Harrison &

Cota (1991) reported a wide range of production estimates for the area, from 105 to 1076 mg C m^{-2} d^{-1}, while Jensen (1999) quoted a mean of 156 mg C m^{-2} d^{-1} for the southern Baffin Bay and Davis Strait.

1.5. Project Objectives

1.5.1. Canada's Three Oceans

The C3O project was a contribution by Fisheries and Oceans Canada to the International Polar Year of 2007/2008. Its goal, in part, was to survey the waters of the Pacific, Arctic, and Atlantic Oceans, producing a 'snapshot' of ocean conditions around Canada during the summers of 2007 and 2008. The 12,000 km cruise track was designed to investigate the interconnectedness between the three ocean basins and target hotspots of biological activity (Carmack et al., 2008; Carmack and McLaughlin, 2011) The overall goal of the project was to systematically evaluate a broad range of physical and biological aspects of the marine environment from the ocean's surface to depths of thousands of metres, measuring water column physical parameters, sediment chemistry, and marine biota from plankton to whales.

The C3O project provided an opportunity to undertake a comprehensive, broad-scale test of the suitability of the regional and shelf-type classification scheme (see section 1.3) as a tool for predicting patterns of primary productivity and export production in the Arctic. It was also an opportunity to create a crucial scientific baseline for future monitoring and assessment of the consequences of global warming on Arctic and Canada's Sub-Arctic Oceans, forming a point of reference from which to compare future studies, and providing important information for policy-makers (Carmack et al., 2008). The C3O sub-project that forms the basis of this thesis focussed on the role of

phytoplankton in the biological pump, and their larger role in the biogeochemistry of the oceans.

1.5.2. Thesis Objectives

- ***Characterization of the structure of the phytoplankton community***

  Both phytoplankton biomass and cell size are indicators of ecological significance. Biomass alone is representative of the standing stock of primary producers; cell size can be used as an indirect indicator, not only of the general species assemblage (functional groups), but also of ecological function within the biological pump.

- ***Determination of net, new and regenerated primary productivity***

  For the purposes of this project, the primary application of nutrient uptake data is to assess the efficiency of the biological pump in a pan-Arctic perspective. The relationship can be numerically represented using a steady state model that incorporates these three 'components' of primary production, derived from the uptake rates of nitrogen and carbon by the phytoplankton community.

- ***Test the validity of the regional and shelf-type classification scheme***

  In this thesis I will address whether the regional classification system is an appropriate tool for establishing a baseline for understanding the current relationship between physical oceanographic processes and phytoplankton dynamics.

- ***Examine the relationship between measured biological and physical parameters***

  I will identify the important bio-physical interactions in each region as a way to provide a more solid basis for predicting future change.

1.6. Thesis Outline

This thesis is organized into five chapters. Chapter 1 (Introduction) has described the role of phytoplankton in marine nutrient cycling, and their role in larger biogeochemical processes in the ocean. The study areas were also introduced here, as well as the specific project objectives. Chapter 2 (Materials and Methods) explains the methodologies used during this project, including sampling sites, sampling techniques, chemical analysis, statistical analyses, and the rational for employing them. Chapter 3 (Results) presents the results of biological and chemical parameters measured, as well as the results of the statistical analysis. Chapter 4 (Discussion and Conclusions) presents a synopsis of the major findings in each region, discusses the most influential phenomena in Arctic waters, and suggests future research possibilities.

CHAPTER 2. MATERIALS AND METHODS

2.1. Sampling Locations

Seawater samples were collected at 42 stations in the northwest Atlantic, Arctic, and northeast Pacific Oceans (Fig. 2.1). It should be noted that the numbers used to identify stations in this thesis differ from the station names used historically and by the C3O program. A list comparing original station names (used in C3O) with those labels used in this thesis is presented in Appendix A. The order of the station numbering does not imply the order in which they were visited: sampling started at station 42 during 2007 and at station 1 in 2008.

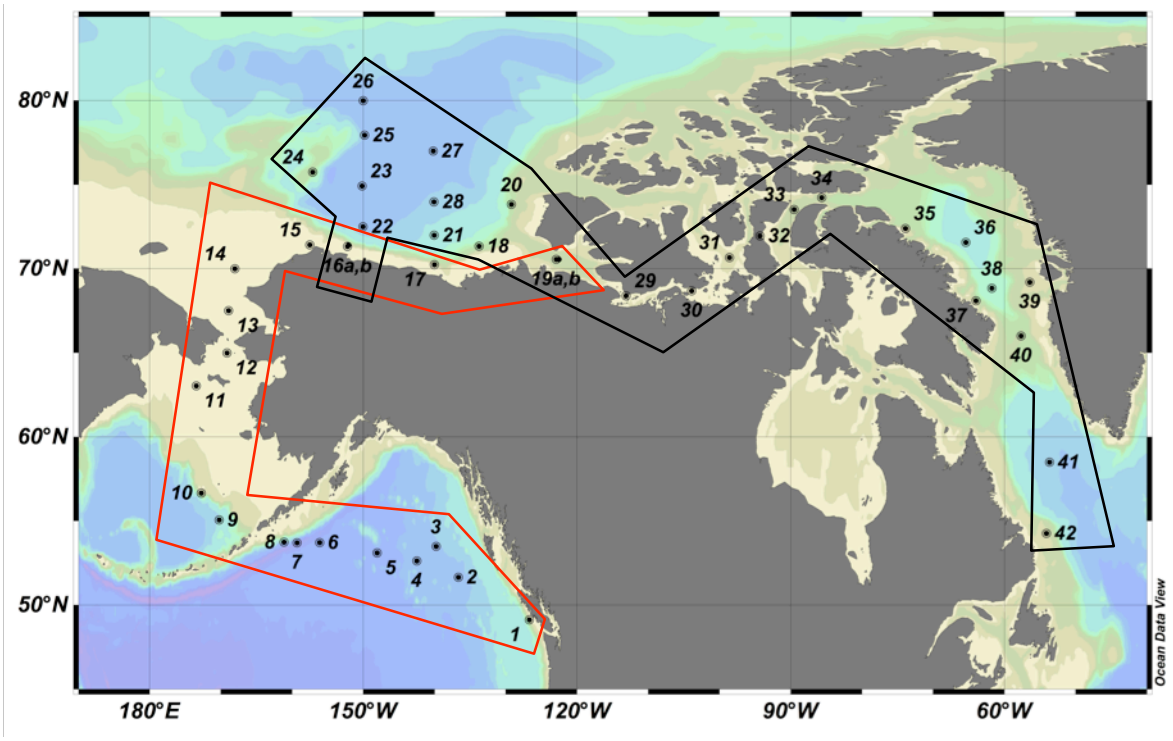

Figure 2.1. Station locations in Arctic and Sub-Arctic waters. Stations within the black polygon were sampled in 2007, while those within the red polygon were sampled in 2008. Stations 16 and 19 were sampled during both years at approximately the same date. Appendix A presents a comparative list of the station labels used in this thesis with the station names used historically and by the C3O program.

In July of 2007, stations 42 to 29 were sampled aboard the CCGS Louis S. St. Laurent in the Labrador Sea, Davis Strait, Baffin Bay, and through the Arctic Archipelago, ending in the Coronation Gulf. During a subsequent cruise, in August 2007, stations 16a, 18, 19a, and 20 to 28 were sampled in the southern Beaufort Sea and Canada Basin, also aboard the CCGS Louis S. St. Laurent. In July 1998, stations 1 to 17, 16b and 19b were sampled in the northeast Pacific, Bering, Chukchi, and southern Beaufort Sea aboard the CCGS Sir Wilfrid Laurier.

2.2. Seawater Sampling

At each station, water samples were collected vertically throughout the euphotic zone using 10 L Niskin bottles. Sampling depths corresponded to the following approximate irradiance levels: 100, 50, 30, 12, 1, and 0.1% of surface irradiance. Seawater samples were collected using a rosette sampling system combined with a CTD profiler equipped with additional sensors (see section 2.3). Seawater samples were collected for the measurement of primary production rates (C and N uptake), and size-fractionated chlorophyll *a*, particulate C and N, biogenic silica (SiO_2), dissolved nutrients (NO_3^-, NH_4^+, urea, $Si(OH)_4$, PO_4^{3-}) and dissolved inorganic carbon (DIC) concentrations, and for the identification of phytoplankton species. In this thesis, I present data corresponding to nutrients, primary production and chlorophyll *a*. The remaining data is presented in Wyatt (2010) and elsewhere.

2.3. Physical Parameters

Water column physical data were collected on-site with a Seabird SB911+ CTD profiler equipped with fluorescence, oxygen, NO_3^- and PAR sensors, and operated by

personnel from the Institute of Ocean Sciences. Ice coverage data were derived from daily ice cover charts generated by the Canadian Ice Service (http://ice-glaces.ec.gc.ca/), as well as personal shipboard observations. Incident PAR data were also collected using a LI-COR LI-190 Quantum Sensor.

2.4. Dissolved Nutrient Concentrations

Samples for dissolved NO_3^-, PO_4^{3-}, and $Si(OH)_4$ concentrations were collected in acid-washed 30 ml polypropylene bottles, immediately frozen at -20°C, and later measured at the University of Victoria using an Astoria II Nutrient Autoanalyzer. Samples for the measurement of dissolved NH_4^+ were collected in 50 ml borosilicate test tubes and analyzed promptly (onboard ship) with the fluorometric method outlined by Holmes et al. (1999) using a Turner Designs TD 700 fluorometer. Dissolved urea samples were collected in 50 ml polypropylene centrifuge tubes, frozen immediately at -20°C, and analyzed at the University of Victoria using the colorimetric method described by Mulvenna & Savidge (1992). Samples for dissolved inorganic carbon (DIC) were collected in 1 L borosilicate bottles, preserved with 200 μL of a saturated mercuric chloride solution, and stored at 4°C. DIC samples were analyzed at the Institute of Ocean Sciences (Fisheries and Oceans Canada) using the coulometric method outlined in Dickson & Goyet (1994).

2.5. Phytoplankton Biomass

Chlorophyll *a* (chl *a*) concentrations were used as a proxy for phytoplankton biomass. Seawater samples were collected in 1 L polypropylene bottles from the same depths as those for primary productivity and all other measurements, filtered immediately

onto 5 μm polycarbonate membrane and 0.7 μm glass fiber filters, and frozen at -20°C until analysis. Filtering in this manner produced separate samples for two phytoplankton size fractions: 0.7 to 5 μm, and >5 μm. Chl *a* was extracted with 90% acetone and analyzed with a Turner Designs 10AU field fluorometer (previously calibrated with pure chlorophyll extract) following the method in Parsons et al. (1984); phaeopigment interference was corrected for by acidification with HCl (1.2 M).

2.6. Net, New and Regenerated Primary Production

Seawater samples were collected in acid-washed 1 L polycarbonate bottles. Samples used for the determination of C uptake were inoculated with a 400 mM $KH^{13}CO_3$ (99% purity) isotope tracer stock with the target ^{13}C enrichment of each sample being <10% of the total ambient dissolved inorganic carbon. For most samples enrichment was between 7 and 9%, except at two locations (stations 27 and 32), where enrichment was as high of 20%. Samples used to determine N uptake rates were inoculated using a 252 μM $Na^{15}NO_3$ stock (98+ % purity) for NO_3^-, $^{15}NH_4Cl$ for NH_4^+ (98% purity), and $(^{15}NH_2)_2CO$ for urea (98% purity), with the final ^{15}N enrichment target for each sample being approximately 10%. Inoculations of ^{13}C and $^{15}NO_3^-$ were done on the same sample, while $^{15}NH_4^+$ and ^{15}N-urea were added to separate samples. Samples were then placed in a temperature-controlled (with flowing surface seawater) on-deck incubators for approximately 24 hours. Incubations were terminated by filtration onto pre-combusted (5 hours at 450°C) 0.7 μm glass fiber filters. Filter samples were dried at 60°C and the isotopic composition of both C and N in the samples (^{12}C:^{13}C and ^{14}N:^{15}N) was measured at the Stable Isotope Facility at the University of California Davis with a PDZ Europa ANCA-GSL elemental analyzer and a PDZ Europa 20-20 isotope ratio mass

spectrometer. Carbon uptake rates were calculated using the methods outlined by Hama et al. (1983), and N uptake rates using equations 1 to 3 of the method outlined by Dugdale & Wilkerson (1986), and f-ratios using the method outlined by Eppley & Peterson (1979).

2.7 Data Presentation

Biological parameters are graphically represented in this thesis in several formats (e.g. discrete data, depth-integrated data). Measurements taken at 6 depths were depth integrated using a trapezoidal integration to produce areal estimates. Depth profiles of relevant data and point values will also be presented as a means to better explain trends. All contour plots were created with Ocean Data View version 4.2.1, and contouring was estimated using DIVA gridding.

2.8. Regional Division of Biological Data

The Shelf-Type classification scheme (see section 1.3) does not include all the stations sampled during this project. Stations that do not fall within the defined regions (Table 2.1 and Fig. 2.2) are excluded from the current statistical discussion. Although all stations sampled will be discussed in this thesis, only those selected will be part of the statistical analysis.

Table 2.1. Regional Definitions based on Shelf Type (as per Carmack & Wassman, 2006). Station locations are presented in Fig. 2.1 and Appendix A.

Region Number and Name	Shelf Type	Associated Stations
Region 1. Northeast Pacific Ocean	Basin	2 to 6
Region 2. Bering & Chukchi Seas	Inflow Shelf	11 to 15
Region 3. South Beaufort Sea	Interior Shelf	16 (a and b) to 18 and 20
Region 4. Canada Basin	Basin	21 to 28
Region 5. Canadian Arctic Archipelago	Outflow Shelf	19 (a and b) and 29 to 34
Region 6. Baffin Bay & Davis Strait	Outflow Shelf/Basin	35 to 40

The southern Bering Sea stations were omitted from the regional grouping on the grounds that they are separated from the rest of the Bering Shelf by the eastern boundary current of the Bering Sea gyre (Stabeno et al., 2009). The coastal stations of the northeast Pacific (stations 1, 8 and 9) are not representative of the oceanic basin, and the Labrador Sea stations (41 and 42) are too far removed geographically from the rest of the study area to be included.

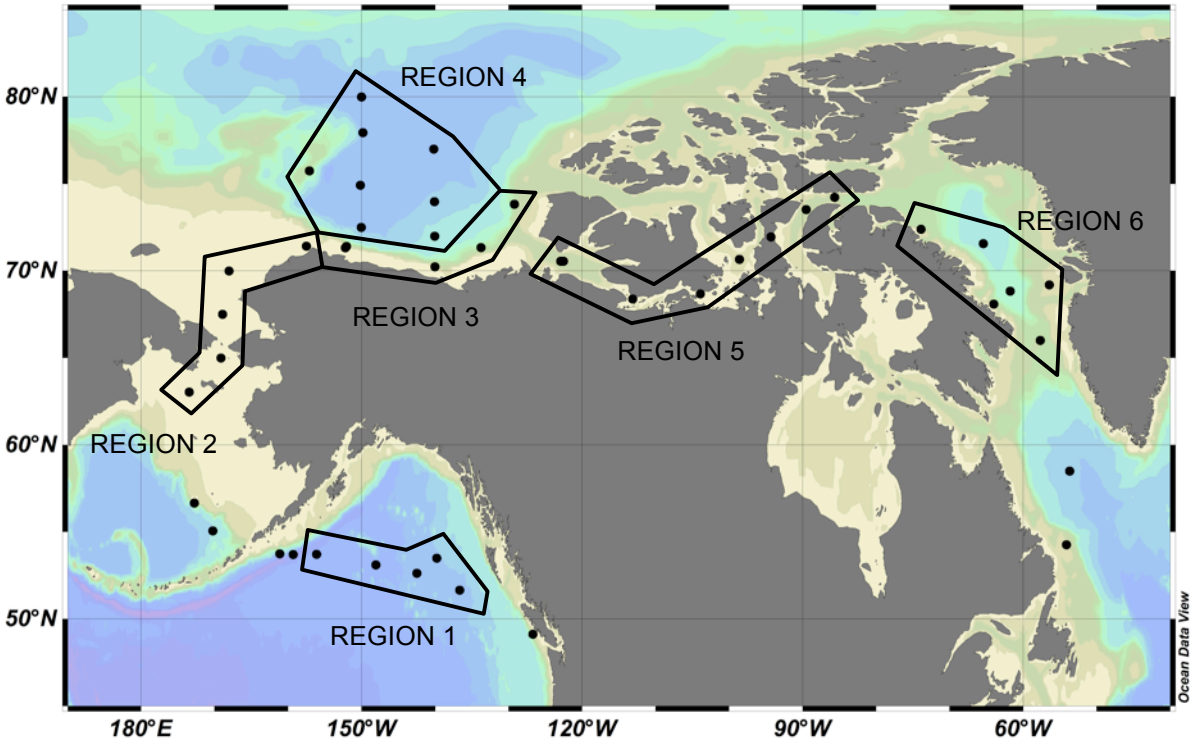

Figure 2.2. Regional divisions based on the Shelf-Type criteria proposed by Carmack & Wassman (2006). Black dots represent all locations sampled during 2007 and 2008.

2.9. Statistical Analysis

A statistical approach was undertaken to verify that the regional groupings actually constrain geographic areas that differ from one another with regards to the

biological properties. The question to be answered is: are the Shelf Type regional selections sufficiently robust to discriminate one region from another?

A one-way ANOVA was used for each parameter (Dependent Variable) being tested, with the Fixed Factor being the geographic Region for all tests. ANOVA was used to determine if there was a statistical differences between regions for each parameter. The parameters tested were: net primary production, f-ratio, total biomass, and percentage of cells >5 μm. Although the ANOVA indicates whether or not a significant difference exists between the means of the parameters based on this regional division, this does not indicate *which* means differ from one another. Tukey's HSD (Honestly Significant Difference) test was used for *post hoc* comparisons to determine which regions differed significantly for the parameters tested. All statistical analyses were carried out using IBM SPSS Statistics, version 19.0.0.

CHAPTER 3. RESULTS

3.1. Overview of Results

Sections 3.2, 3.3 and 3.4 present a region-by-region description of depth-integrated phytoplankton biomass (total and percentage of cells larger than 5 μm), primary production (net primary production and f-ratios), and dissolved nutrient data. Section 3.5 presents the results of the statistical analysis of the regional model introduced in section 1.3, with a brief interpretation of the results. Regional averages for each biological parameter are presented in Appendix B (Table B.2) , and average nutrient concentrations are presented in Appendix C (Table C.2).

3.2. Phytoplankton Biomass

3.2.1. Northeast Pacific Ocean

In the offshore northeast Pacific (stns 2 to 6), biomass ranged from 11.9 to 32.0 mg chl *a* m^{-2} (Figs. 3.1 and 3.3A), and the percentage of cells >5 μm varied from 19 to 43% (Figs. 3.2 and 3.3A). In contrast, the coastal portions of the northeast Pacific (stations 1, 7 and 8) were characterized by higher biomass (12.7 to 51.8 mg chl *a* m^{-2}) and a higher proportion of larger cells (30 to 71%) in the phytoplankton assemblage.

3.2.2. Bering and Chukchi Seas

The Southern Bering Sea (stns 9 and 10) was characterized by higher biomass (18.9 and 43.5 mg chl *a* m^{-2}, respectively) than the stations 11 and 12 in the north (16.8 and 17.9 mg chl *a* m^{-2}) (Figs. 3.1 and 3.3A), but a lower percentage of cells >5 μm (11 and 14% compared to 44 and 46%) (Figs. 3.2 and 3.3A). In the Chukchi Sea (stns 13 to

15), biomass ranged from 40.7 to 61.1 mg chl *a* m^{-2}, with larger cells representing 72 to 89% of the assemblage.

3.2.3. South Beaufort Sea

The South Beaufort Sea (stns. 16 to 18, and 20) was characterized by lower chlorophyll *a* concentrations (6.8 to 31.8 mg chl *a* m^{-2}) than those in the Chukchi Sea (Figs. 3.1 and 3.3B). We sampled station 16 in both 2007 (August 3) and 2008 (July 23), with very different chl *a* concentrations: 9.5 mg m^{-2} and 30% cells >5 μm in 2007, compared to 31.8 mg chl *a* m^{-2} and 86% cells >5 μm in 2008 (Figs. 3.2 and 3.3B).

3.2.4. Canada Basin

The Canada Basin (stns 21 to 28) was characterized by the lowest chlorophyll *a* concentrations in the entire study area, ranging from 4.7 to 10.4 mg chl *a* m^{-2} (Figs. 3.1 and 3.3B), and by the presence of smaller cells (only 12 to 33% cells >5 μm) (Figs. 3.2 and 3.3B).

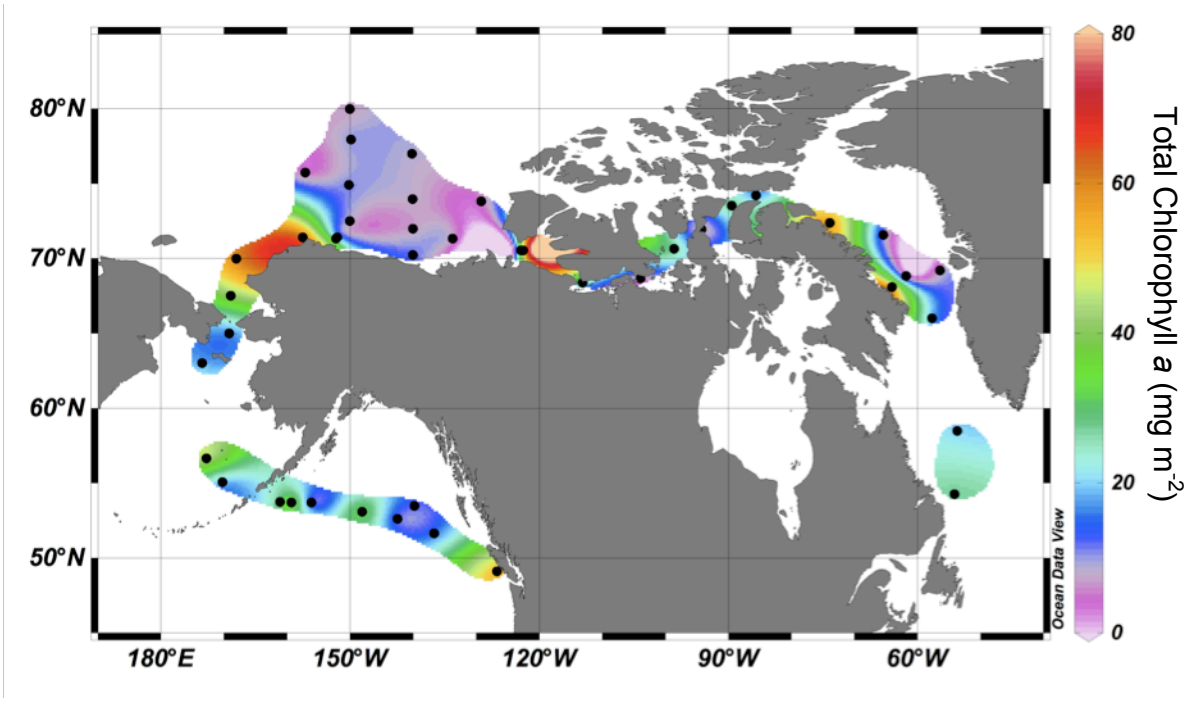

Figure 3.1. Depth-integrated total chlorophyll *a* concentrations (>0.7 µm) in Arctic and Sub-Arctic waters during the summers of 2007 and 2008. Interpolation between stations was done with Ocean Data View 4.2.1 DIVA gridding. Black dots represent station locations.

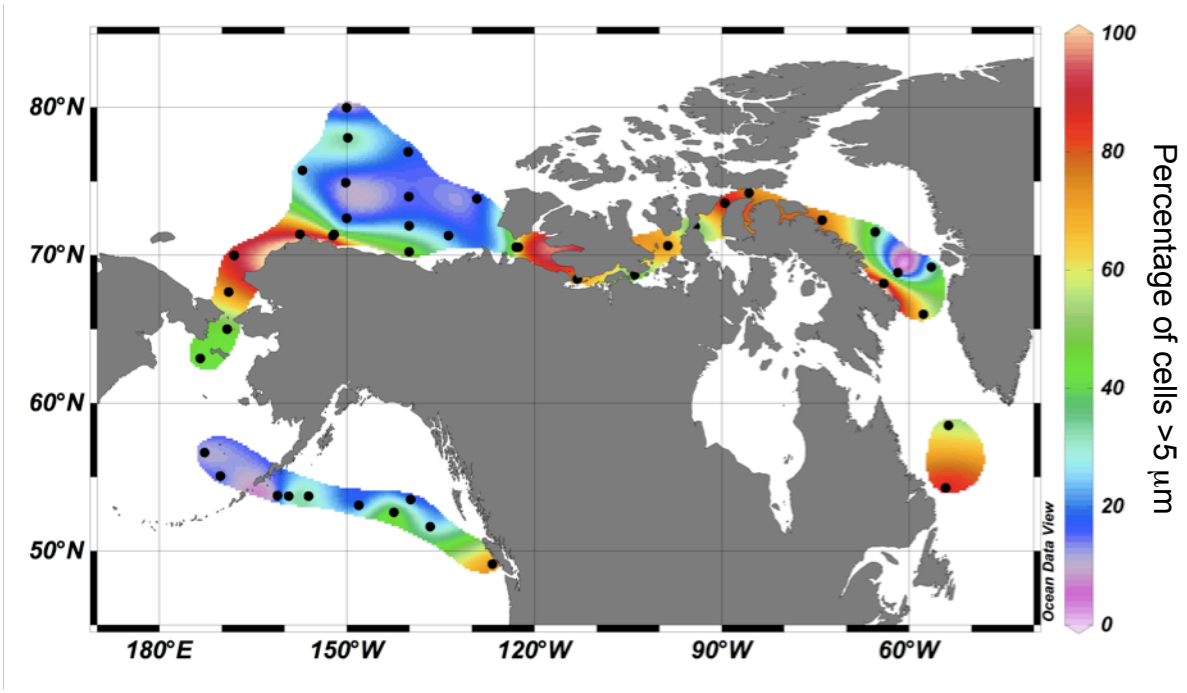

Figure 3.2. Percentage of depth-integrated chlorophyll *a* attributed to cells >5 µm in Arctic and Sub-Arctic waters during the summers of 2007 and 2008. Interpolation between stations was done with Ocean Data View 4.2.1 DIVA gridding. Black dots represent station locations.

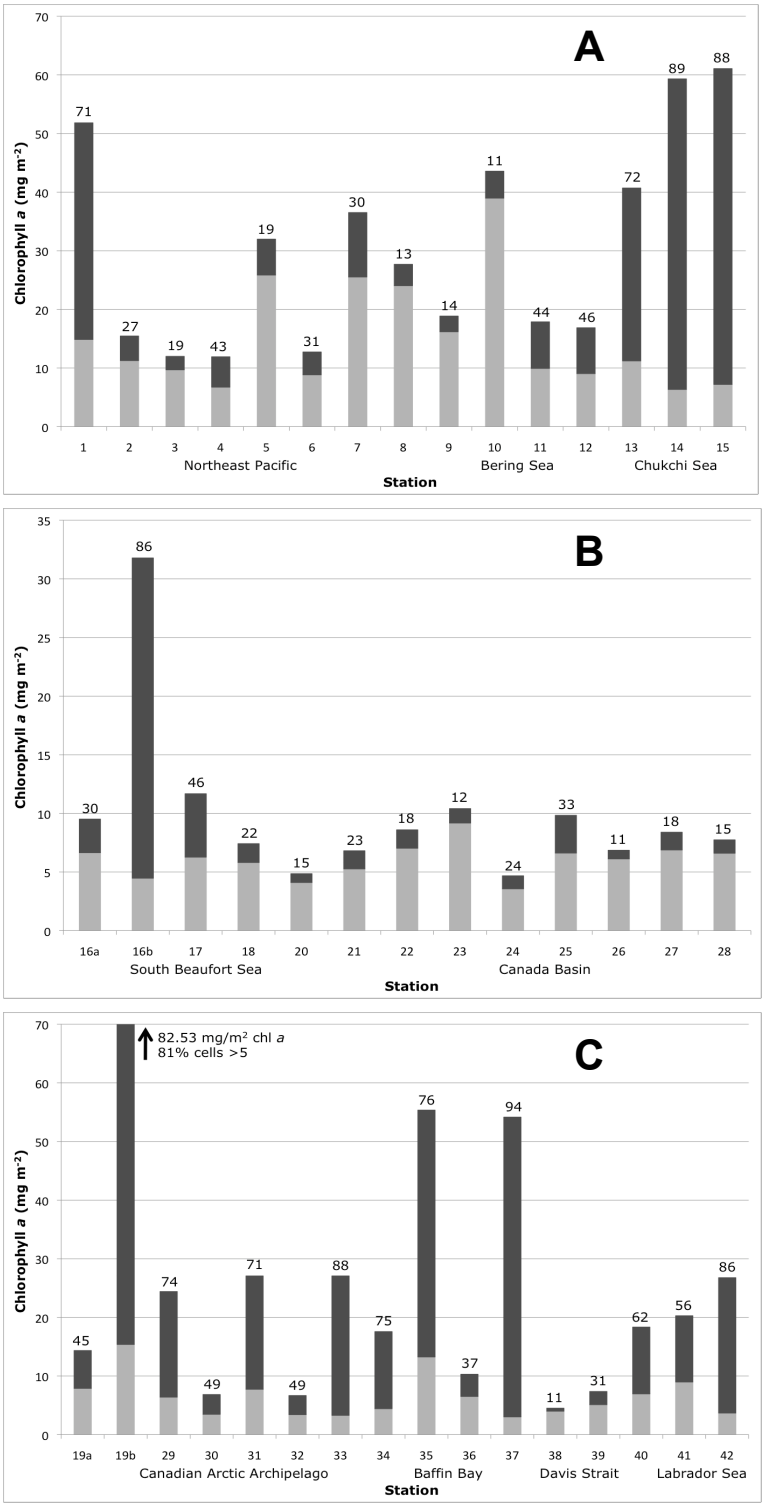

Figure 3.3. Depth-integrated phytoplankton biomass in the A: Northeast Pacific, Bering and Chukchi Seas; B: Beaufort Sea and Canada Basin; and C: Canadian Arctic Archipelago, Baffin Bay, Davis Strait, and Labrador Sea. Stations are represented by both station number and general geographic location; note that stations 16a and 16b are labelled in the opposite order to those stations in Wyatt (2010). The dark grey portion represents the proportion of the phytoplankton assemblage represented by larger (>5 μm), the light gray portion represents cells <5 μm. Numbers above bars indicate the percentage of cells >5 μm. Note that the scale of figure B is 1/2 that of the A and C.

3.2.5. Canadian Arctic Archipelago

Chlorophyll a concentrations in the Canadian Arctic Archipelago (stns 19, and 29 to 34) varied from 6.7 to 82.5 mg chl *a* m^{-2} (Figs. 3.1 and 3.3C), with larger cells representing 45 to 88% of the assemblage (Figs. 3.2 and 3.3C). As was the case for Stn 16, we also sampled Stn 19, in the Amundsen Gulf, during both years (July 28, 2007 and July 28, 2008) and observed large biological variability. In 2007 biomass at Stn 19 was 14.3 mg chl *a* m^{-2} with 45% of cells >5 μm, and in 2008 biomass was 82.5 mg chl *a* m^{-2} with 81% of cells >5 μm.

3.2.6. Baffin Bay and Davis Strait

Phytoplankton biomass in Baffin Bay and Davis Strait (stns 35 to 40) varied from 4.5 to 55.4 mg chl *a* m^{-2} (Figs. 3.1 and 3.3C), the highest chl *a* values occurring along the coast of Baffin Island (stns 35 and 37). The proportion of the assemblage represented by larger cells varied between 11 and 94%, the highest of these values also occurring at stns 35 and 37 and the lowest at stn 38 in southern Baffin Bay (Figs. 3.2 and 3.3C).

3.2.7. Labrador Sea

Chlorophyll *a* concentrations in the Labrador Sea (stns 41 and 42) were 26.8 and 4.5 mg chl *a* m^{-2} at the offshore stn 41 and 55.4 mg chl *a* m^{-2} (Figs. 3.1 and 3.3C) at station 42 located closer to shore. Larger cells dominated the biomass at both stations (56 and 86%, respectively) (Figs. 3.2 and 3.3C).

3.3. Net Primary Production

3.3.1. Northeast Pacific Ocean

In the offshore Northeast Pacific (stns 2 to 6), NPP rates ranged from 64 to 730 mg C m^{-2} d^{-1} (Figs. 3.4 and 3.6A), with variable depth-integrated f-ratios, from 0.19 to 0.91 (Figs. 3.5 and 3.6A).The coastal portions of the region were characterized by NPP values from 578 mg C m^{-2} d^{-1} near the Aleutian Island chain (stns 7 and 8) to 6182 mg C m^{-2} d^{-1} off the coast of Vancouver Island (stn 1).

3.3.2. Bering and Chukchi Seas

In the southern Bering Sea (stns 9 and 10), NPP rates were 366 and 641 mg C m^{-2} d^{-1}; in the north Bering, NPP rates were 164 mg C m^{-2} d^{-1} at stn 11 and 1069 mg C m^{-2} d^{-1} at station 12 (Figs. 3.4 and 3.6A). The Chukchi Sea stns were higher overall than those in the Bering Sea, ranging from 1026 to 1581 mg C m^{-2} d^{-1} with associated f-ratios varying from 0.63 to 0.86 (Figs. 3.5 and 3.6A).

3.3.3. South Beaufort Sea

The South Beaufort Sea (stns 16 to 18, and 20) was characterized by NPP rates ranging from 19 to 194 mg C m^{-2} d^{-1} (Figs. 3.4 and 3.6B)and f-ratios from 0.12 to 0.53 (Figs. 3.5 and 3.6B). Stn 16, sampled in both 2007 and 2008, had a NPP rate of 195 with an f-ratio of 0.20 in 2007, and a net primary production rate of 158 mg C m^{-2} d^{-1} with an f-ratio of 0.53 in 2008.

3.3.4. Canada Basin

The Canada Basin (stns 21 to 28) was characterized by the lowest overall NPP rates in the study, ranging from 32 to 103 mg C m^{-2} d^{-1} (Figs. 3.4 and 3.6B), with f-ratios from 0.10 to 0.56 (Figs. 3.5 and 3.6B).

3.3.5. Canadian Arctic Archipelago

NPP rates in the Canadian Arctic Archipelago (stns 19, and 29 to 34) were variable (14 to 1520 mg C m^{-2} d^{-1}) (Figs. 3.4 and 3.6C) with f-ratios ranging from 0.09 to 0.61 (Figs. 3.5 and 3.6C). Stn 19 was sampled in both years of the project; in 2007 NPP was 2334 mg C m^{-2} d^{-1} with an f-ratio of 0.16, and in 2008 NPP was 14 mg C m^{-2} d^{-1} with an f-ratio of 0.09.

3.3.6. Baffin Bay and Davis Strait

NPP in Baffin Bay and Davis Strait (stns 35 to 40) varied between 181 and 1818 mg C m^{-2} d^{-1} (Figs. 3.4 and 3.6C), with f-ratios ranging from 0.18 to 0.48 (Figs. 3.5 and 3.6C).

3.3.7. Labrador Sea

At the offshore Labrador Sea station 41, NPP was 343 mg C m^{-2} d^{-1} (Figs. 3.4 and 3.6C) with an f-ratio of 0.25 (Figs. 3.5 and 3.6C); at the coastal station (42), NPP was 1751 mg C m^{-2} d^{-1}.

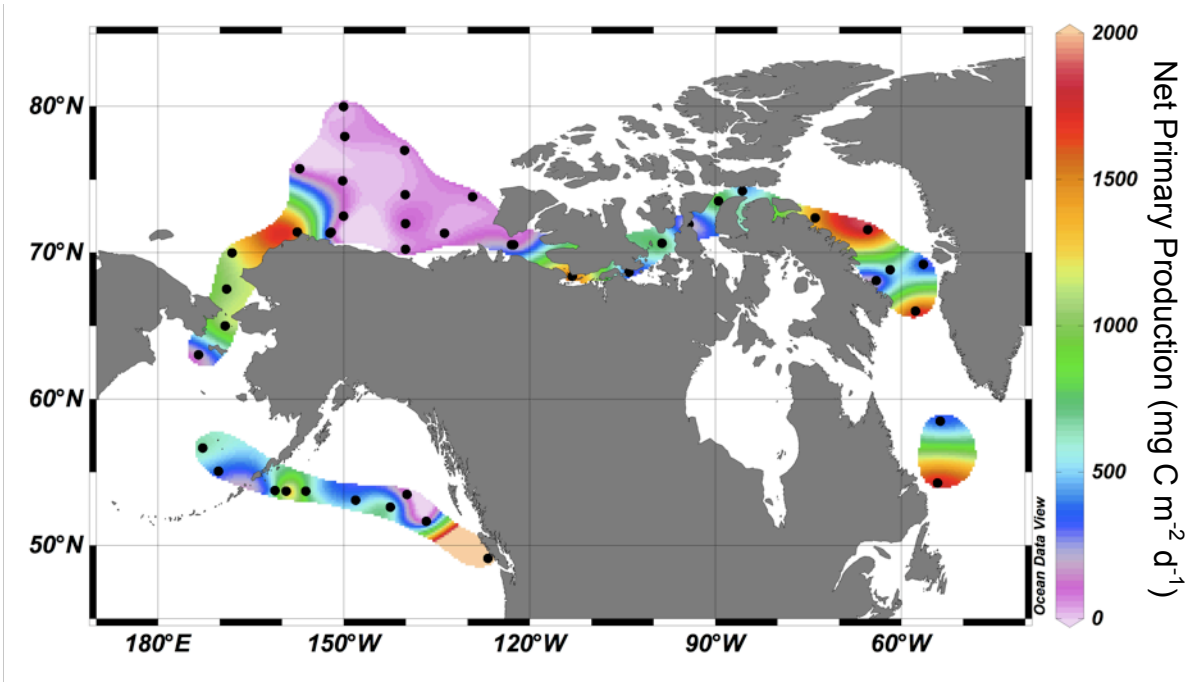

Figure 3.4. Depth-integrated primary production in Arctic and Sub-Arctic waters during the summers of 2007 and 2008. Interpolation between stations was done with Ocean Data View 4.2.1 DIVA gridding. Black dots represent station locations.

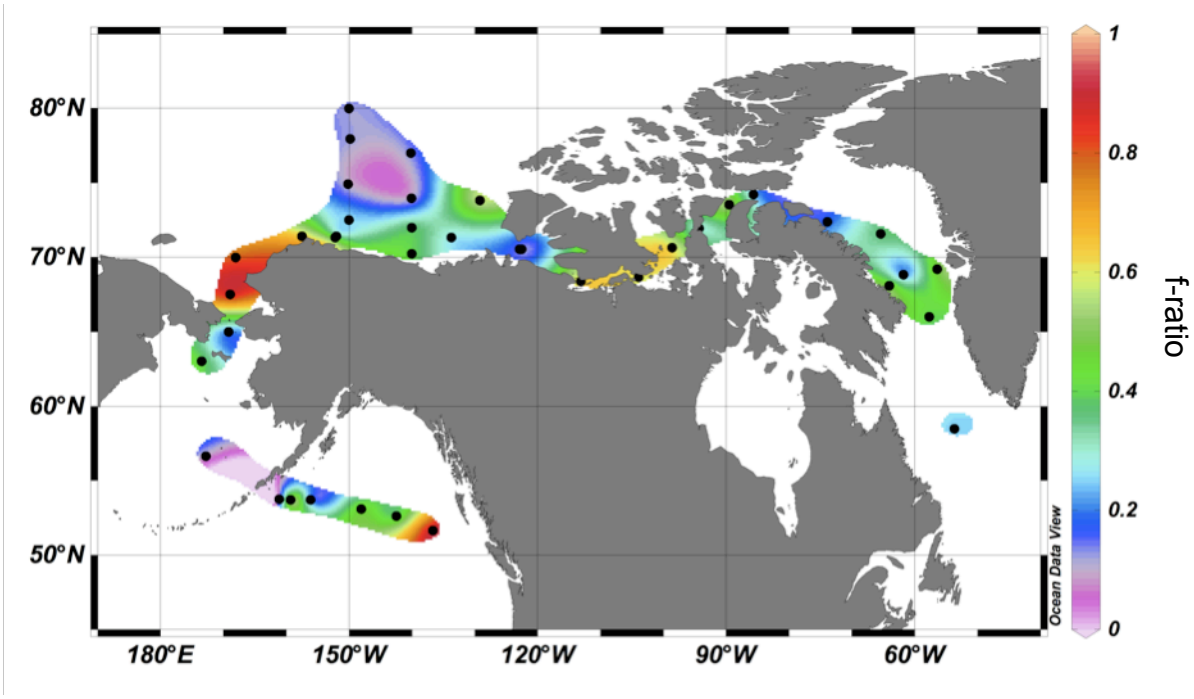

Figure 3.5. Depth-integrated f-ratios in Arctic and Sub-Arctic waters during the summers of 2007 and 2008. Interpolation between stations was done with Ocean Data View 4.2.1 DIVA gridding. Black dots represent station locations.

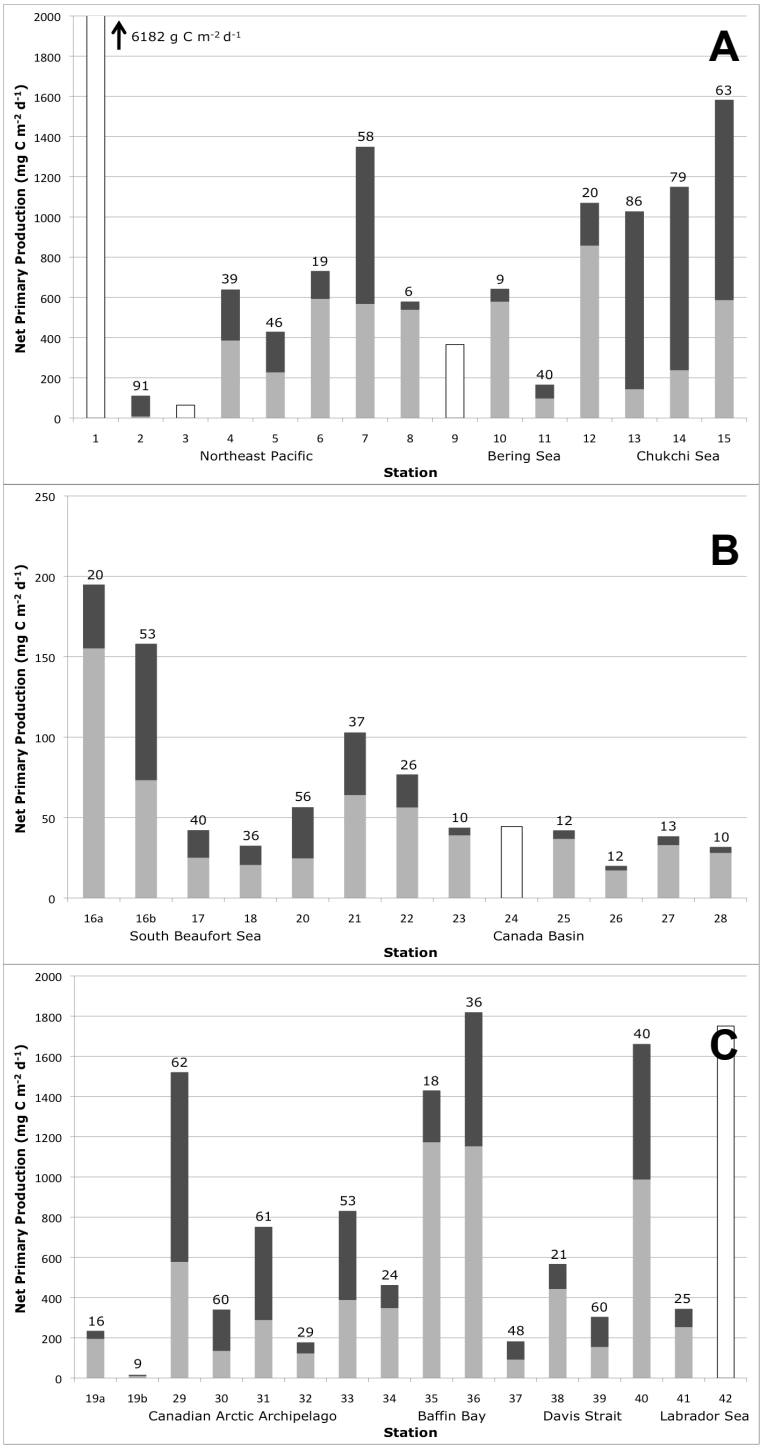

Figure 3.6. Depth-integrated net, new, and regenerated primary production in the A: Northeast Pacific, Bering and Chukchi Seas; B: Beaufort Sea and Canada Basin; and C: Canadian Arctic Archipelago, Baffin Bay, Davis Strait, and Labrador Sea. Stations are represented by both station number and general geographic location; note that stations 16a and 16b are labelled in the opposite order to those stations in Wyatt (2010). The dark grey portion represents new production, the light grey portion represents regenerated production. Numbers above bars indicate the proportion of net primary production attributed to new production. Hollow bars represent only net primary production. Note that the scale of figure B is 1/8 that of the A and C.

3.4. Dissolved Nutrient Concentrations

3.4.1. Nitrate

The highest areal NO_3^- concentrations were found in the Northeast Pacific (Fig. 3.7). The stations in the central Alaska Gyre exhibiting the highest concentrations (up to 2112.9 mmol m^{-2} at stn 4). In the Bering and Chukchi Seas, dissolved NO_3^- ranged from 173.7 to 567.7 mmol m^{-2}, similar to those levels found in the Beaufort Sea with the exception of the much lower concentrations measured at station 16a (2007). In the Canada Basin, nitrate was higher in the deeper central basin (up to 770.3 mmol m^{-2} at stn 23) and lower approaching the shallower Beaufort Shelf (from 173.2 mmol m^{-2} at stn 21). Nitrate concentrations were similar in the Canadian Arctic Archipelago, Baffin Bay, Davis Strait, and Labrador Sea, ranging from 96.6 mmol m^{-2} at stn 30, to 518.7 mmol m^{-2} found at stn 39. In the Northeast Pacific Ocean, NO_3^- concentrations were as high as 20 μmol L^{-1} in the top 5 m of the water column, a marked contrast to surface NO_3^- in the Canada Basin and South Beaufort Sea where NO_3^- exhaustion was evident in surface waters (Fig. 3.8).

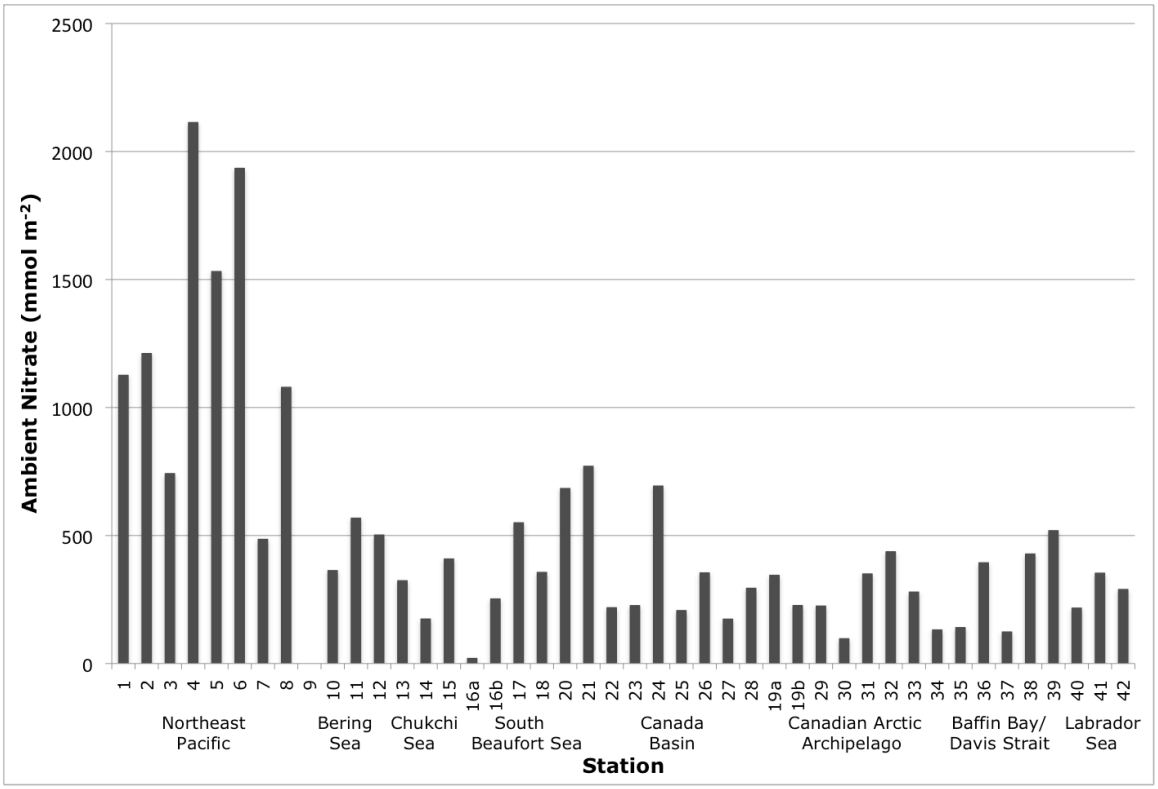

Figure 3.7. Depth-integrated nitrate concentrations in Arctic and Sub-Arctic waters for 2007 and 2008, by station and geographic area. Note that stations 16a and 16b are labelled in the opposite order to those stations in Wyatt (2010).

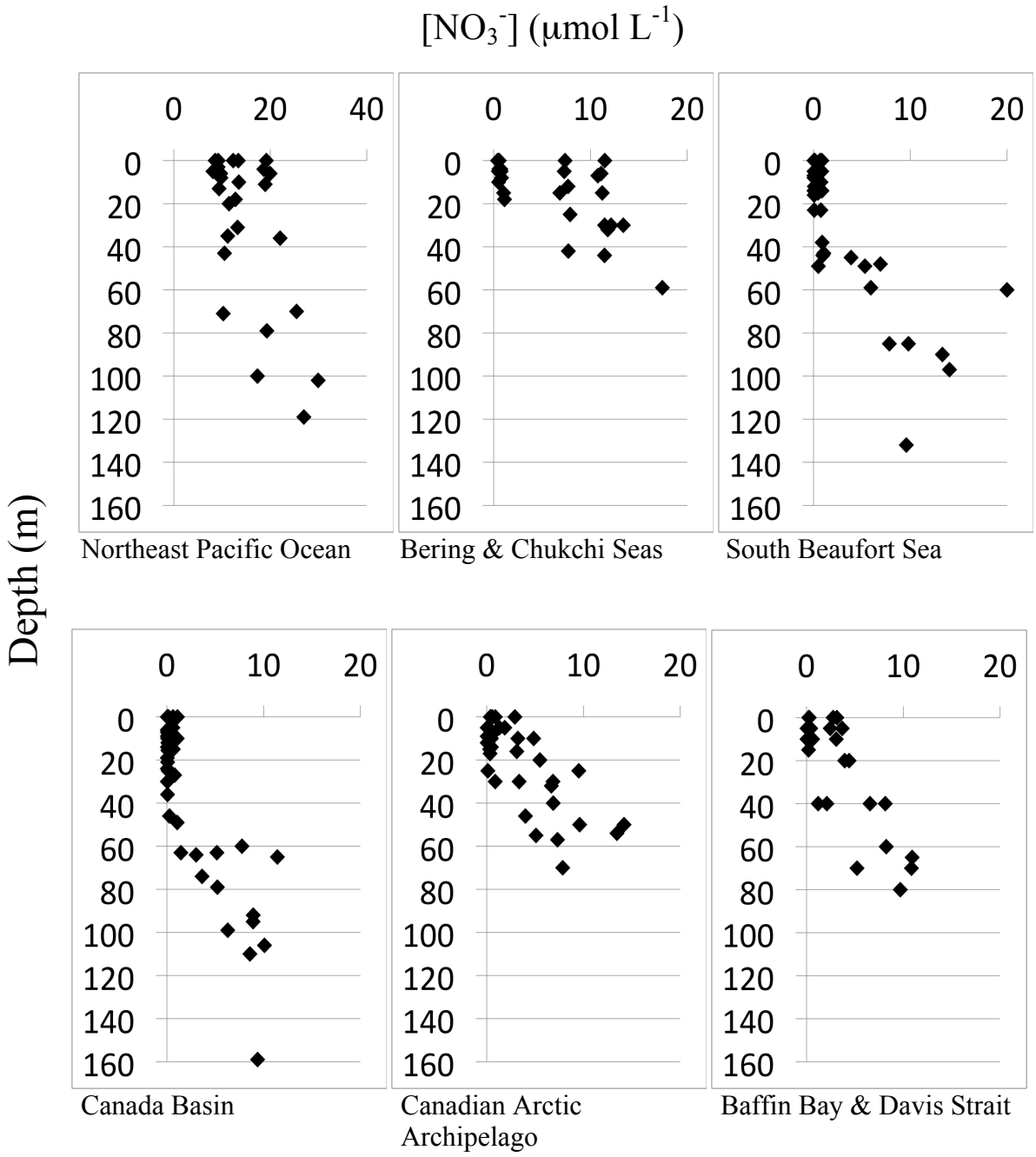

Figure 3.8. Regional dissolved NO_3^- profiles. Note that the scale for NO_3^- concentrations in the Northeast Pacific Ocean is twice that of the other regions.

3.4.2. Ammonium and Urea

Ammonium concentrations varied between 13.6 and 44.7 mmol m^{-2} in the central northeast Pacific, increasing to 248.2 mmol m^{-2} near the Aleutian Islands (Fig. 3.8A). Ammonium levels ranged between 23.3 and 151.0 mmol m^{-2} in the Bering and Chukchi Seas, and dropping off to between 3.5 and 118.3 mmol m^{-2} in the south Beaufort Sea, Canada Basin, and Canadian Arctic archipelago. In Baffin Bay and Davis Strait, NH_4^+ concentrations were mostly between 9.1 and 28.4 mmol m^{-2}, with a high value of 105.6 mmol m^{-2} at stn 39. Urea concentrations were highly variable in all locations, with the highest concentration at stn 22 in the Canada Basin (60.8 mmol m^{-2}), and the lowest at stn 14 in the Chukchi Sea (7.1 mmol m^{-2}) (Fig. 3.8B). Urea concentrations were variable throughout the water column (Fig. 3.11), and NH_4^+ was depleted at all depths and stations in the Canada Basin and South Beaufort Sea (Figs. 3.10).

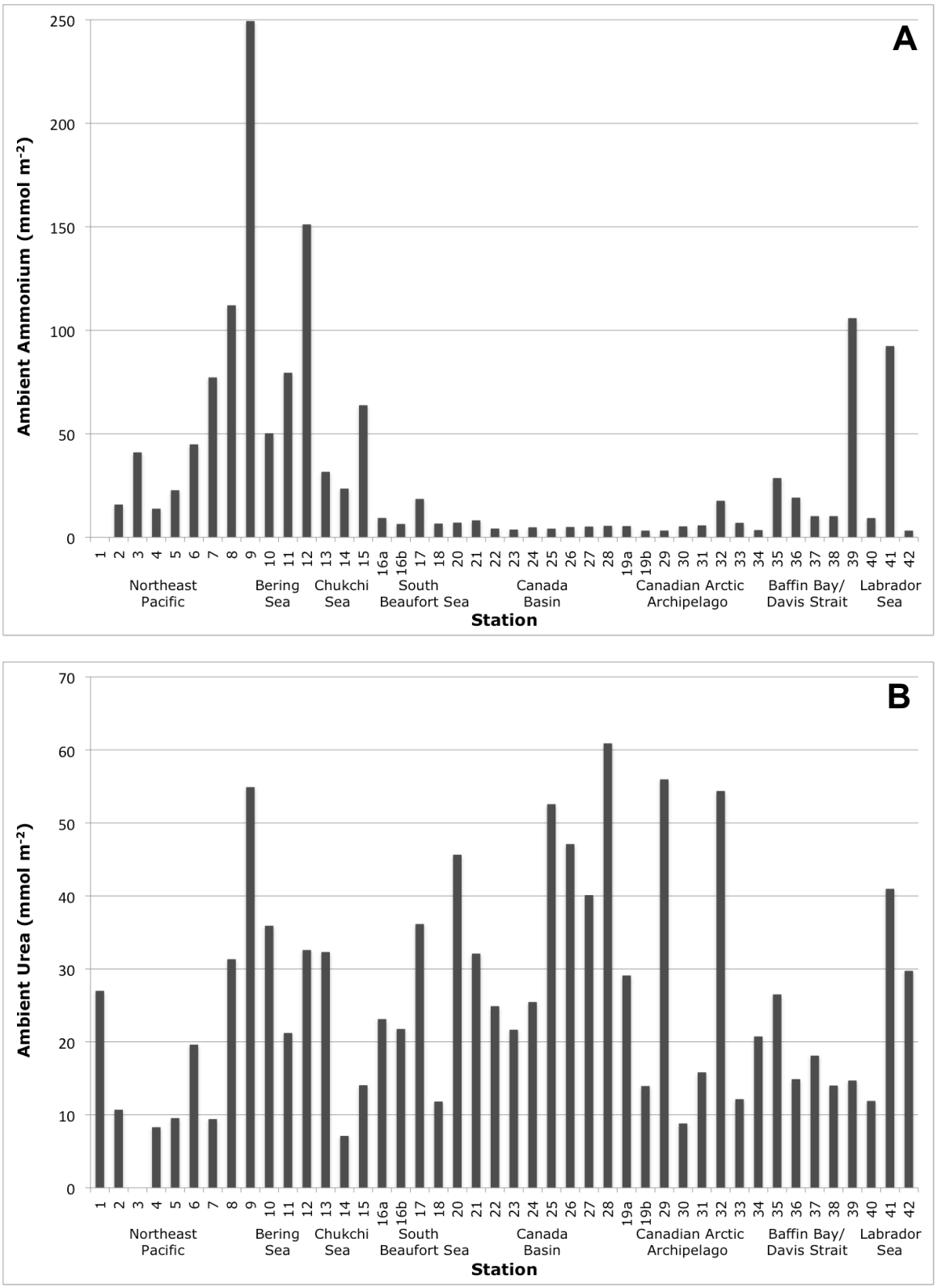

Figure 3.9. Depth-integrated A: ammonium, and B: urea concentrations in Arctic and Sub-Arctic waters for 2007 and 2008, by station and geographic area. note that stations 16a and 16b are labelled in the opposite order to those stations in Wyatt (2010).

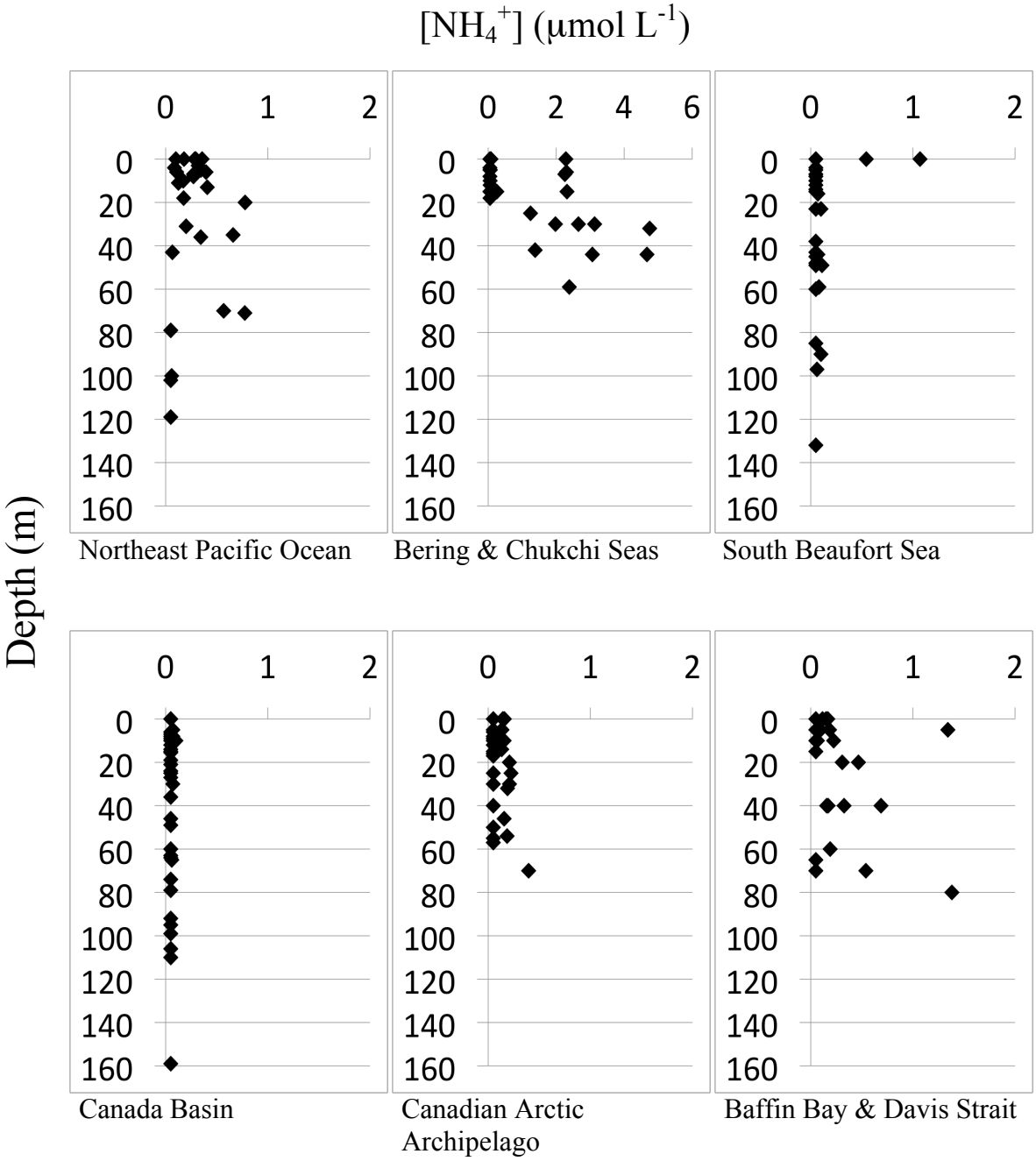

Figure 3.10. Regional dissolved NH_4^+ concentrations. Note that the range of NH_4^+ concentrations in the Bering & Chukchi Seas is 3 times that of the other regions.

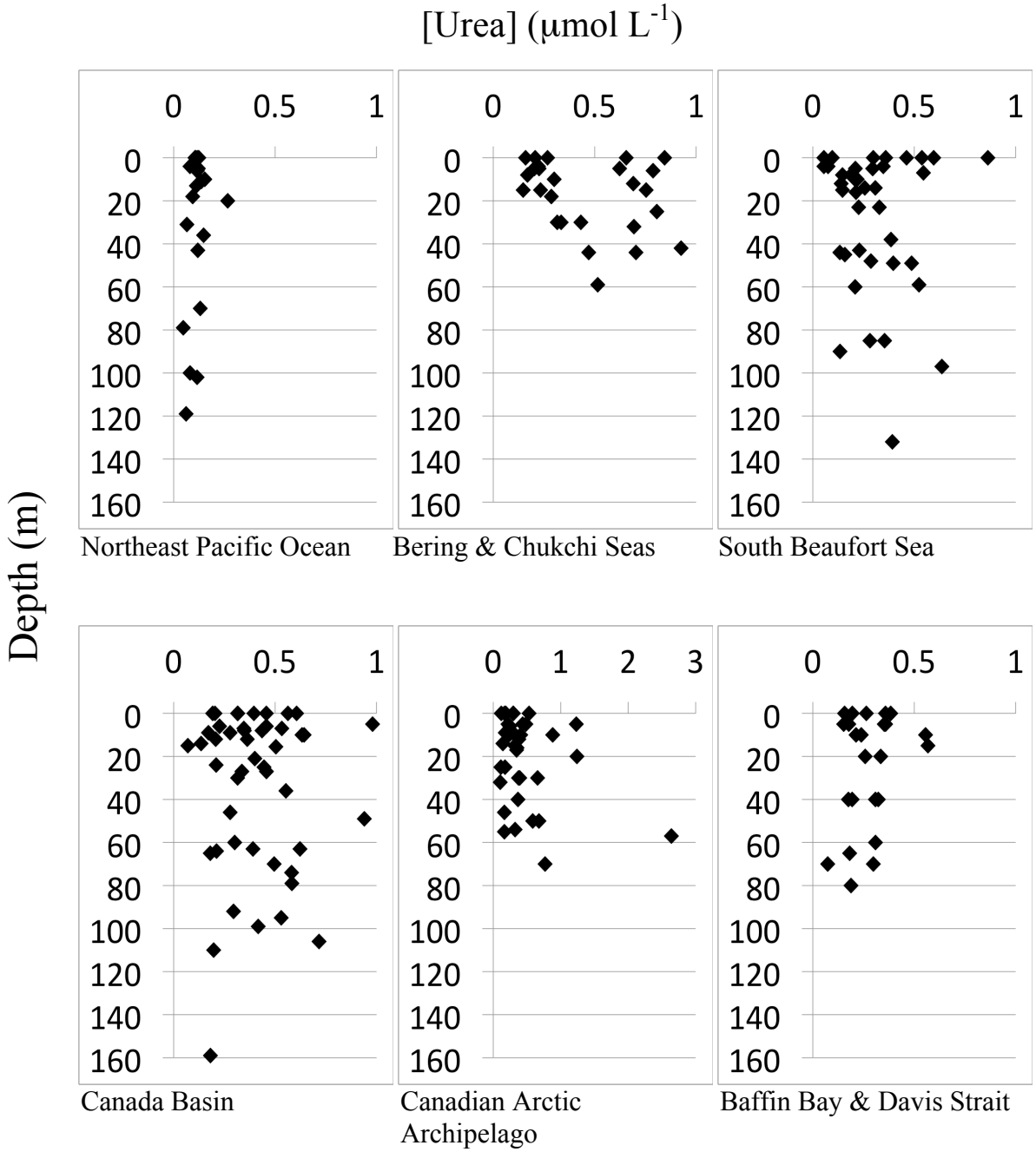

Figure 3.11. Regional dissolved urea profiles. Note that the scale for urea concentrations in the Canadian Arctic Archipelago is 3 times that of the other regions.

3.4.3. Silicic Acid

Silicic acid concentrations in the Northeast Pacific were the highest found during the project, ranging from 813.4 to 2982.3 mmol m^{-2} (Fig. 3.12). In the Bering, Chukchi and Beaufort Seas levels ranged from 370.2 to 2448.0 mmol m^{-2}, and similar in the Canada Basin with the exception of higher values found in the deeper basin (up to 2448.0 mmol m^{-2}). In the Canadian Arctic Archipelago, $Si(OH)_4$ concentrations were variable (ranging from 244.0 to 1535.3 mmol m^{-2}), and lower still in Baffin Bay, Davis Strait and the Labrador Sea (130.5 to 555.8 mmol m^{-2}). $Si(OH)_4$ concentrations showed similar trends to those of nitrate in the Canada Basin and South Beaufort Sea (depleted in surface waters but not exhausted), and variable in other regions (Fig. 3.13).

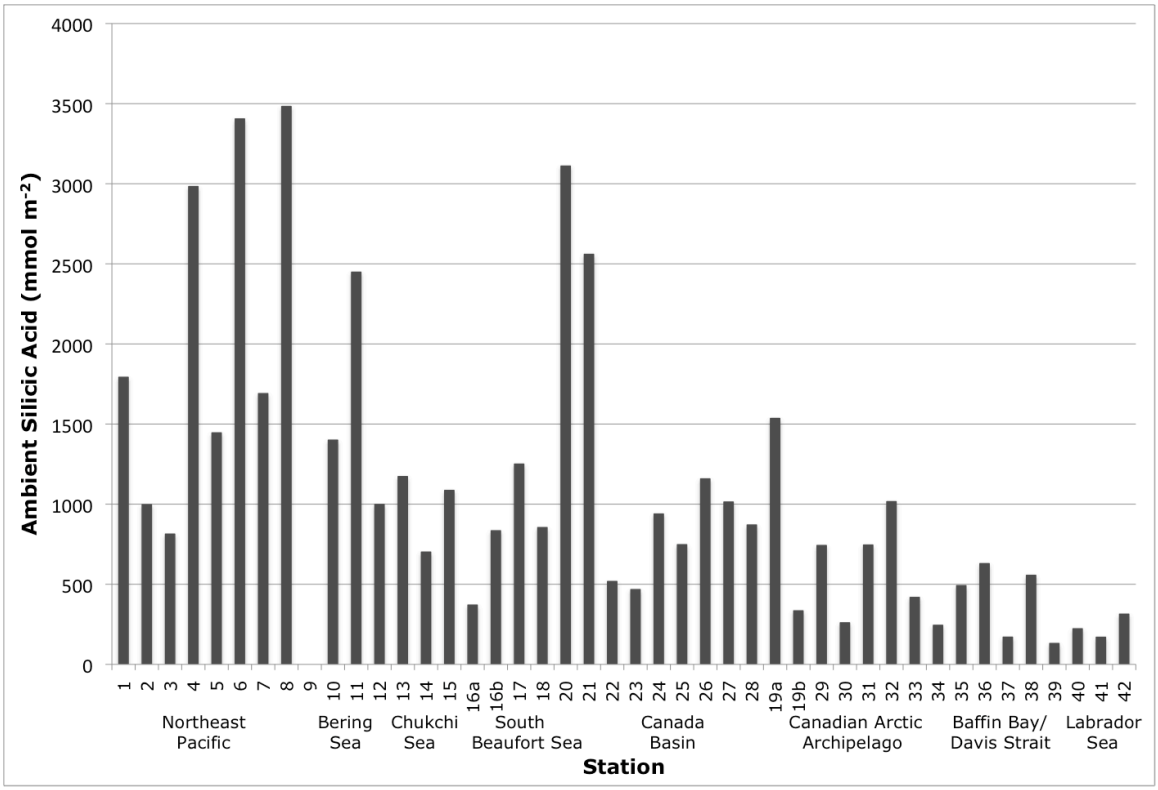

Figure 3.12. Depth-integrated silicic acid concentrations in Arctic and Sub-Arctic waters for 2007 and 2008, by station and geographic area. Note that stations 16a and 16b are labelled in the opposite order to those stations in Wyatt (2010).

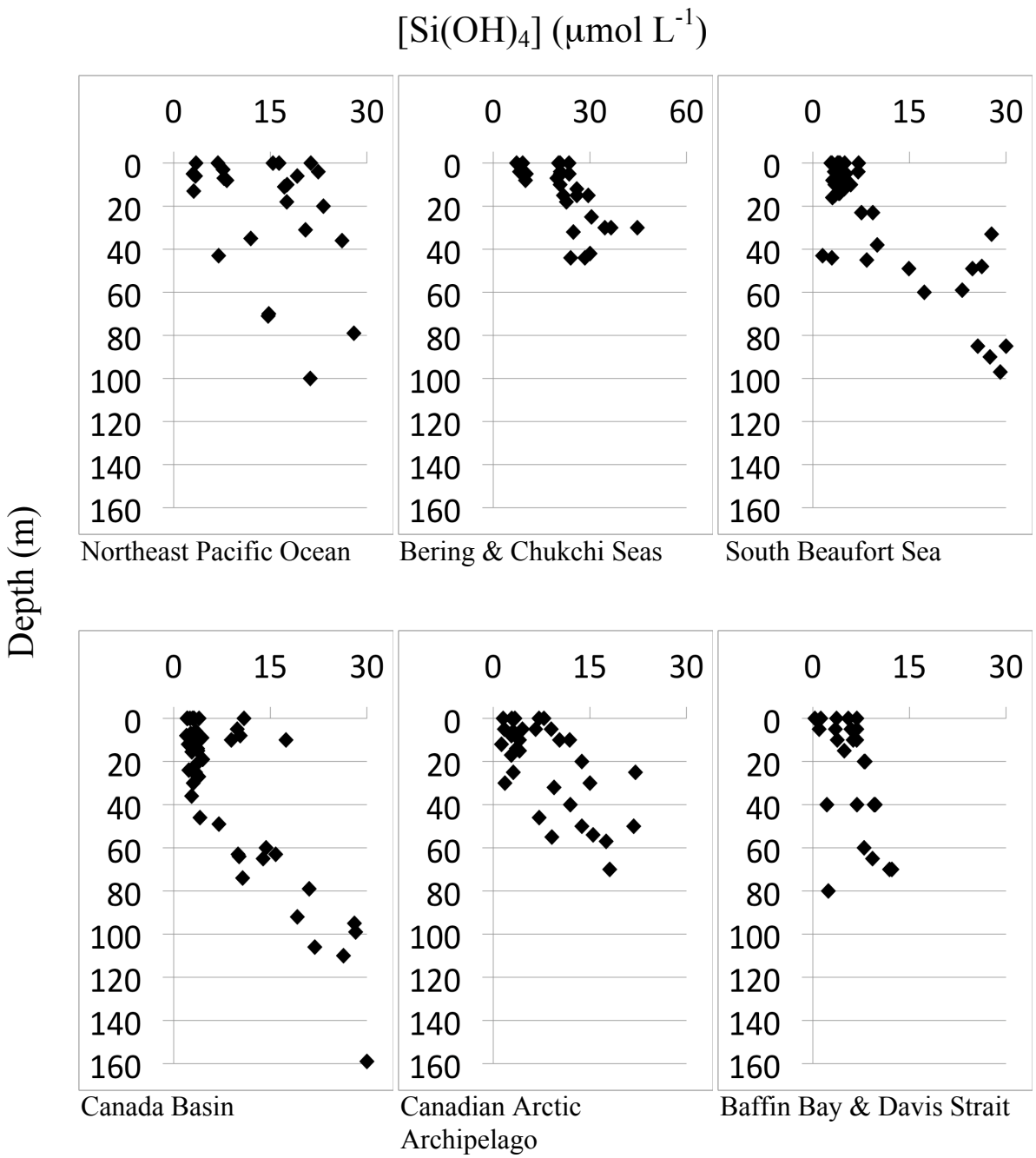

Figure 3.13. Regional dissolved $Si(OH)_4$ profiles. Note that the scale for $Si(OH)_4$ concentrations in the Bering & Chukchi Seas is twice that of the other regions.

3.5. Statistical Analysis

3.5.1. Biomass and Percentage of Cells >5 µm

The mean total biomass of all regions were not significantly different from one another, but - with p only slightly larger than 0.05 - only marginally so (ANOVA, $F_{5,31,0.05} = 2.426$, $p = 0.057$, Effect Size = 0.281; Table 3.1). The only significant difference existed between The Bering & Chukchi Seas (Region 2) and the Canada Basin (Region 4). There was, however, a significant difference in mean percentage > 5 µm between regions (ANOVA, $F_{5,31,0.05} = 6.524$, $p = 0.000$, Effect Size = 0.513; Table 3.1). Mean percentages > 5 µm in the Bering Strait and Chukchi Sea, and Canadian Arctic Archipelago were significantly higher than those in the Northeast Pacific and Canada Basin.

3.5.2. Net Primary Production and f-ratios

There were significant differences in mean NPP between regions (ANOVA, $F_{5,31,0.05} = 5.619$, $p = 0.001$, Effect Size = 0.682; Table 3.1). The Bering Strait and Chukchi Sea (Region 2), and Baffin Bay and Davis Strait (Region 6) had significantly higher mean NPP than both the South Beaufort Sea (Region 3) and Canada Basin (Region 4), which were not significantly different from each other. The mean NPP of the Northeast Pacific (Region 1), Bering Strait and Chukchi Sea, Canadian Arctic Archipelago (Region 5), and Baffin Bay and Davis Strait were not significantly different from one another. The mean f-ratios of all regions were not significantly different from one another (ANOVA, $F_{5,31,0.05} = 1.801$, $p = 0.144$, Effect Size = 0.237; Table 3.1).

Table 3.1. ANOVA Results. The F score is the ratio of variance between regions to the variance within each region; a higher value essentially represents a greater difference between regions for the particular parameter. The p-value states whether there is a significant difference between Regions, based on the significance threshold (95% certainty). The Effect Size shows the proportion of the difference (or lack thereof) attributed to the parameters being divided up by Region in the manner that they were. For example, there is 95% certainty that 68% of all the Net Primary Production measurements made during the study differed significantly between regions based solely on the Shelf-Type divisions that were assigned in this study.

Dependent Variable	Fixed Factor	$F_{5,31,0.05}$	p-value	Effect Size
Total Biomass	Region	2.426	0.057	0.281
Percentage of cells >5 μm		6.524	0.000	0.513
Net Primary Production		5.619	0.001	0.682
f-ratio		1.801	0.144	0.237

3.5.3. Interpretation of Statistical Results

The statistical analysis shows that the Shelf-Type regional division proposed here is a reasonably appropriate way of dividing up the study area. Although f-ratios were not significantly different between regions, net primary production was significantly different, as was the percentage of cells >5 μm. Total biomass was not significantly different between regions, but the result was only marginally non-significant (p-value of 0.057 compared to the statistical threshold of 0.05).

Figure 3.14 and 3.15 show mean total chl *a* and primary production per region, and using the graph alone it is difficult to determine why a significant difference (albeit slight) exists between regions for some parameters. The reason is that variability *within* each region is quite large in some cases compared to the variability *between* regional means (see Figs. 3.14 and 3.15). For example, in Baffin Bay & Davis Strait, standard error is over 40% of the mean in terms of total chl *a,* and regional means are close enough to be statistically similar. When the sample size increases, the estimate of the mean is based on more information and becomes more accurate, so standard error of the mean decreases. The small number of samples is probably the reason for the large spread

of values here, and increased sampling in each region would decrease this variability considerably.

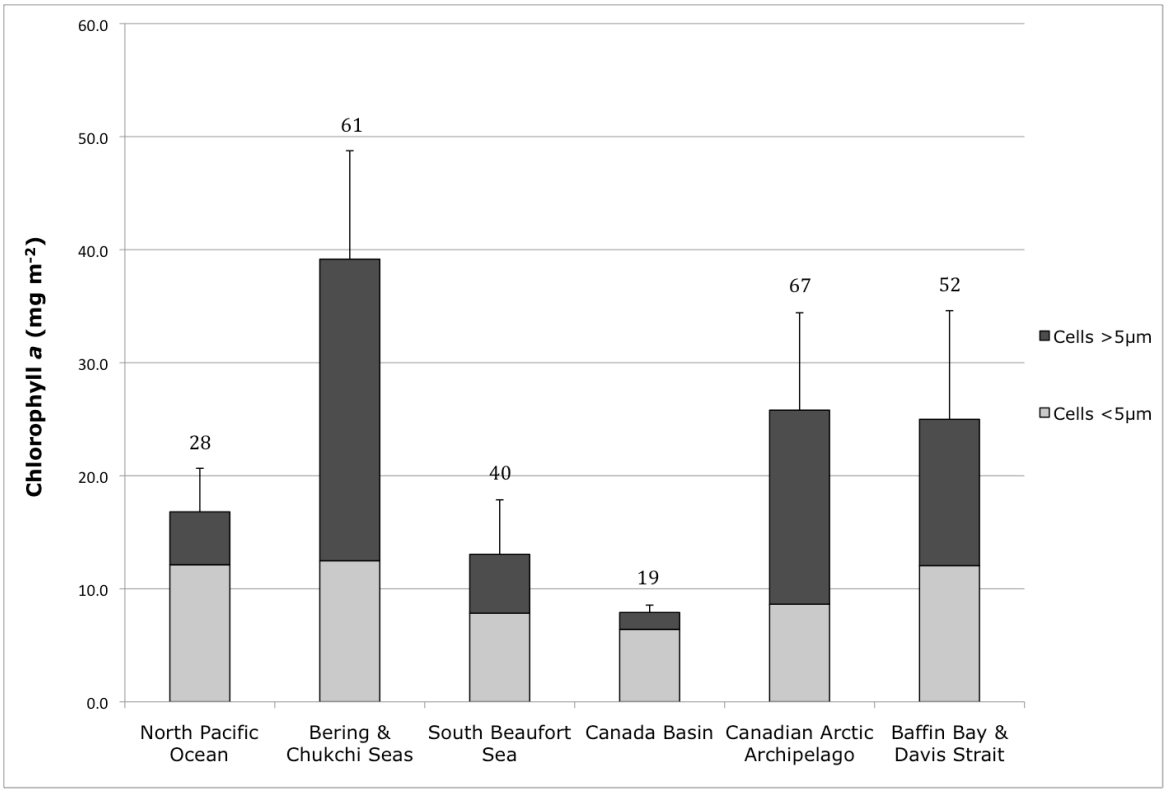

Figure 3.14. Mean phytoplankton biomass (chl *a*) by geographic region. The total height of the bar represents the average total biomass for each region, the dark grey portion represents the proportion of the phytoplankton assemblage represented by larger (>5 μm) cells, and the light gray portion represents cells <5 μm. Numbers above bars indicate the proportion (%) of the phytoplankton biomass comprised of cells >5 μm. Error bars represent the standard error of the mean of total biomass.

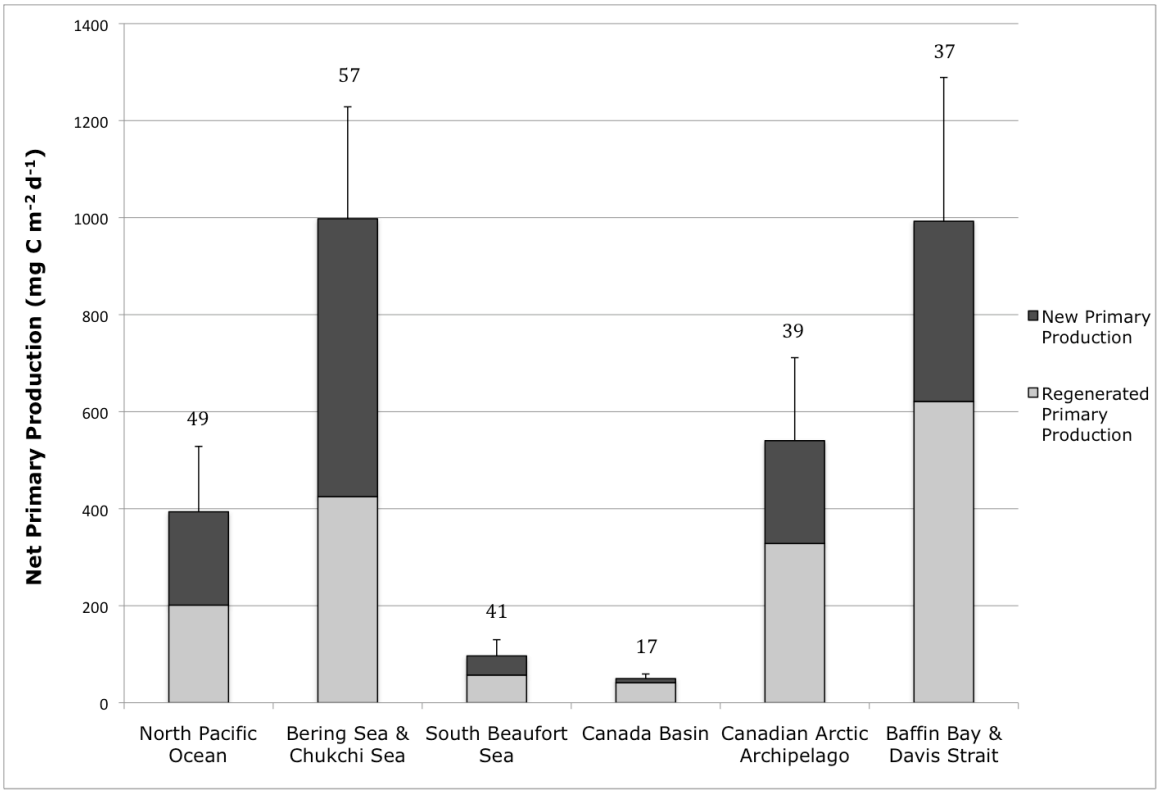

Figure 3.15. Mean depth-integrated net, new, and regenerated primary production by geographic region. The total height of the bar represents the average net primary production for each region, the dark grey portion represents new production, and the light grey portion represents regenerated production. Numbers above bars indicate the proportion (%) of net primary production attributed to new production. error bars represent the standard error of mean of net primary production.

CHAPTER 4. DISCUSSION AND CONCLUSIONS

4.1. Discussion of Phytoplankton Production In Arctic and Sub-Arctic Marine Waters

4.1.1. Northeast Pacific Ocean

Based on primary production estimates, Boyd & Harrison (1999) suggested that the Sub-Arctic Northeast Pacific could be broadly split into two distinct regions: coastal and oceanic.

At ***stn 1***, on the shelf break off the west coast of Vancouver Island (Fig. 2.1; Table A.1), the euphotic zone extended down to 79 m, with NO_3^- concentrations ranged from ~1 μmol L^{-1} in the top 10 m, to >22 μmol L^{-1} below 50 m. The $Si(OH)_4$ profile followed a similar trend, ranging from 9 to 13 μmol L^{-1} in the top 10 m, to >30 μmol L^{-1} below 50 m. NPP at stn 1 was the highest measured during the study (6182 mg C m^{-2} d^{-1}) and the high phytoplankton biomass (51.8 mg chl *a* m^{-2}) was comprised primarily (71%) of larger cells. Although an f-ratio was not determined at this location due to a lack of the necessary dissolved NH_4^+ data, the phytoplankton assemblage was comprised primarily of large cells, and this together with the high NO_3^- drawdown fits with the model of a system dominated by new production (see section 1.1.3).

Stations close to the Aleutian Islands were heavily influenced by Alaskan coastal water, and thus not grouped together with the oceanic stations (although bottom depth was >4000 m). They were also influenced by a cyclonic eddy, ***stn 7*** being on the east side of the eddy and ***stn 8*** close to the center. Although NO_3^- and $Si(OH)_4$ at both stations were replete, NPP at stn 7 was more than twice as high as that at stn 8 (1348 compared to

578 mg C m^{-2} d^{-1}, respectively) with the f-ratio an order or magnitude higher (0.58) at stn 7 compared to 0.06 at stn 8. Biomass was also higher at stn 7 than at stn 8 (36.5 compared to 27.7 mg chl *a* m^{-2}), and comprised of a greater proportion of larger cells (30 compared to 13%). The position of each station in terms of its proximity to the center of the eddy may have been a factor in explaining this difference. It is possible that the outside of the eddy (stn 7) was characterized by cells from within eddy, fed by nutrients upwelled from depth in the center and eventually forced to the outside where the higher chlorophyll levels were observed.

The oceanic Sub-Arctic Northeast Pacific is a high-nitrate, low-chlorophyll (HNLC) region (Boyd & Harrison, 1999; Dugdale & Wilkerson, 1991), and this is reflected in both the high NO_3^- concentrations, and the low phytoplankton biomass, compared to other areas visited in the study. ***Stns 2 to 6*** were characterized by euphotic zones of 70 to 102 m depth and abundant dissolved NO_3^- and $Si(OH)_4$. Despite abundant dissolved nutrient concentrations (NO_3^- concentrations at stations 4 to 6 were the highest recorded during this study), NPP was an order of magnitude lower than that found at stn 1 (ranging from 64 to 730 mg C m^{-2} d^{-1}) and f-ratios were variable (0.19 to 0.91), although the mean f-ratio for these stations was 0.49. Phytoplankton biomass ranged from 11.9 to 30 mg chl *a* m^{-2}, the assemblage being comprised primarily (>57%) of smaller cells. The high NO_3^- and low NH_4^+ concentrations, combined with a mean f-ratio <0.50 suggests a system dominated by regenerated production, and most likely low particle export from the euphotic zone. This supports conclusions by Varela & Harrison (1999) and Peña & Varela (2007) that phytoplankton assemblages comprised of smaller cells utilized NH_4^+ as the primary N source in the oceanic stations in this region. NPP values

reported here also fall within the range quoted by Harrison et al. (1999) of 300 to 600 mg C m^{-2} d^{-1}.

4.1.2. Bering and Chukchi Seas

Stns 9 and 10, in the southern Bering Sea, were not included in the statistical analysis due to their distance from the other stations in this region, but do deserve to be mentioned here. These stations were sampled just off the shelf at a depth of 2441 m (stn 9) and just on the continental shelf at a depth of 143 m (stn 10). Both NPP and biomass were higher at stn 10, perhaps due to shelf break upwelling.

The north Bering Sea ***stations (11 and 12)*** were located in 74 and 49 m of water, respectively, with euphotic zones that went nearly to the ocean floor at both stations. The nutrient regime in the north Bering Sea is determined by three distinct flow regimes (Fig. 1.1). The Bering Shelf Water, located some distance from the coast, influences the local nutrient regimes. This water mass is derived from the westernmost end of the Alaska Current and runs north across the central Bering Shelf. The Anadyr Water, which typically stays close to the Eurasian coast, does sometimes flow eastward into the vicinity of stn 11, carrying with it a different chemical signature than that of the Bering Shelf Water (Kostianoy et al., 2005). At stn 11, off the southeast corner of St. Lawrence Island, $[NO_3^-]$ was <1 μmol L^{-1} and NH_4^+ was undetectable (<0.05 μmol L^{-1}) in the top 15m of the euphotic zone, but increased below this depth. The nutrient regime at stn 12, south of the Bering Strait, was markedly different with $[NO_3^-]$ ~11 μmol L^{-1} throughout a well-mixed euphotic zone, and $[NH_4^+]$ was >2 μmol L^{-1} in the upper 15 m. Although phytoplankton biomass was only 6% greater at stn 11, NPP at stn 12 was more than 5x higher (1069 compared to 164 mg C m^{-2} d^{-1}), while the f-ratio at both stations was <0.50.

The depletion of all N species at stn 11 was possibly indicative of a very rapid biomass turnover. The f-ratio of <0.50 and the dominance of smaller cells also supports this scenario. At stn 12, the concentration of all N species were abundant throughout the euphotic zone ($[NO_3^-]$ in excess of 10 μmol L^{-1}), and although NPP was much higher than at stn 11, the f-ratio at was also <0.50 and the assemblage was also comprised primarily (54%) of smaller cells. Walsh et al. (1989) reported significant grazing pressure by copepods, primarily on diatoms (92% of the assemblage) in the vicinity of stn 12, which would indicate a discrepancy between that study and this one assuming that diatoms in the Walsh study are representative of a larger size fraction. Perhaps, despite a nutrient load capable of supporting larger siliceous cells, grazing pressure was heavy enough to draw down the population during this study. While possible, this scenario is contrary to the findings by Lovvorn et al. (2005) that large amounts of organic material does end up settling to the ocean floor, owing to low grazing pressure. Regardless, the NPP data reported here from both stns 11 and 12 do agree with primary production estimates by Springer & McRoy (1993) of ~500 mg C m^{-2} d^{-1} and f-ratios ranging from 0.10 to 0.50.

During the summer months, 60% of the water flowing north through Bering Strait is derived from the Anadyr current, the south Chukchi Sea being flooded with nutrient rich water, particularly in the southwest (Walsh et al., 1989). The remaining flow through the Strait is a combination of Alaska Coastal Current and Bering Shelf Water. ***Stns 13, 14 and 15*** were located on the Chukchi shelf at depths of 51, 495, and 127 m, respectively, and with a nutrient regime heavily influenced by water flowing through the Bering Strait. Stn 15 was located at the head of Barrow Canyon and subject to periodic upwelling (Hill

& Cota, 2005). Nitrate concentrations were ~7 μmol L^{-1} throughout the euphotic zone at stn 13, just north of the Bering Strait, but depleted (<1 μmol L^{-1}) in the surface 10 m and increasing to ~12 μmol L^{-1} below this depth at both stns 14 and 15. Silicic acid concentrations showed similar trends: >18 μmol L^{-1} throughout the euphotic zone at stn 13, but comparably lower (<8 μmol L^{-1}) in the 10 m at stns 14 and 15. NPP rates were some of the highest found in the study, ranging from 1026 mg C m^{-2} d^{-1} at stn 13 to 1581 mg C m^{-2} d^{-1} at stn 15. At all three stations, f-ratios were >0.50. Biomass values here were also among the highest found in this study, with all assemblages comprised of primarily larger cells.

Stn 14, in the northeast Chukchi Sea, was similar to stn 13 with regard to NPP and f-ratio, but exhibited a higher standing stock of phytoplankton (59.3 compared to 40.7 mg chl *a* m^{-2}), larger cells making up a larger proportion of the biomass (89 compared to 72%). Stn 14 was sampled within sight of the edge of receding seasonal ice (Environment Canada, 2011a; personal observation), and the higher biomass may have been attributed to stabilization of the water column in the presence of freshwater inputs from melting ice (Alexander & Niebauer, 1981). Previous estimates of NPP and biomass in the Chukchi Sea are diverse. Bates et al. (2005) reported NPP rates as low as 340 mg C m^{-2} d^{-1} during the summer months on the Chukchi shelf, while Hansell et al. (1993) measured mid-shelf rates as high 6000 mg C m^{-2} d^{-1}. Although these studies were conducted over a decade apart, they show the variability of NPP rates found the Chukchi Sea, and the rates reported in this study fall somewhere in the middle of that range. The effects of seasonal ice melt have been shown to play a significant role in the timing and magnitude of phytoplankton blooms (Alexander & Niebauer, 1981), which can be brief in nature,

illustrating the importance of timing for studying phytoplankton dynamics in the Chukchi Sea. Gosselin et al. (1997) reported NPP rates of 2570 mg C m^{-2} d^{-1} in the northwest Chukchi Sea during the summer of 1994, while Cota et al. (1996) reported 30 mg C m^{-2} d^{-1} only a year earlier in the same area. In the latter study, NO_3^- depletion in surface waters and the comparatively lower NPP led them to conclude that they had just missed the bloom. During this thesis, surface NO_3^- depletion (<1 μmol L^{-1}) was observed in the southeastern Chukchi at stn 14, but NPP was >1000 mg C m^{-2} d^{-1} with a corresponding f-ratio of 0.89, typical of conditions present in a nutrient-rich environment. This indicates a system driven by NO_3^- as an N source, suggesting an early and active phytoplankton bloom, as opposed to a post-bloom scenario brought on by NO_3^- limitation. The presence of a phytoplankton assemblage consisting primarily (89%) of larger cells, which is often indicative of NO_3^- driven systems, also supports this scenario. The salinity of the top 10 m was 29 PSU, as opposed to 32 PSU below this depth, suggesting stratification due to fresh water inputs, most likely due to sea ice melt.

Stn 15, over Barrow Canyon, was also sampled within sight of the ice edge. Surface NO_3^- depletion and fresh water layer also existed at this location, which was characterized by an f-ratio >0.50, a phytoplankton assemblage comprised primarily (88%) of larger cells, and an NPP of 1581 mg C m^{-2} d^{-1}. Stn 15 was located at a site of periodic upwelling from the deeper waters of the Canada Basin (Woodgate et al., 2005). In addition to nutrient inputs of Pacific origin from the Bering Strait, nutrients in the area have been shown to be of Atlantic origin, presumably upwelled through the canyon and contributing to NPP values of 8000 mg C m^{-2} d^{-1} in the vicinity of Barrow Canyon (Hill & Cota, 2005). It is possible that upwelling may have been due to northerly winds which

were present at the time of sampling in this study (Environment Canada, 2011b), and higher NO_3^- concentrations at the base of the euphotic zone at both stations, compared to the surface water, suggest that this may have been a possibility as phytoplankton drew down nutrient concentrations near the surface but not at depth.

4.1.3. South Beaufort Sea

This region consists of the waters of the Beaufort Sea east of Point Barrow and overlying the shelf and slope to a depth of 1000 m. The water of the Alaska Coastal Current follows the Alaska coast, supporting productivity in the Eastern Chukchi so that by the time it gets to Point Barrow, it has lost most of its nutrient load (Hill & Cota, 2005) prior to entering the south Beaufort Sea. Minor upwelling through marine canyons events are known to occur along the Beaufort shelf (Carmack & Macdonald, 2002), but the majority of the water in the Beaufort Sea - especially off-shelf - is a combination of surface water from the Chukchi Sea and Beaufort Gyre, in addition to riverine inputs (Hill & Cota, 2005)

Stns 16a and 16b were sampled at the same location, east of Point Barrow (Fig. 1.2A) on August 3, 2007 and July 23, 2008, respectively. Note that stations 16a and 16b as discussed here are in the opposite order to those stations discussed in Wyatt (2010). During both years, the euphotic zone was stratified, with salinities in the top 10 m ranging from 23 to 29 PSU, and increasing gradually to 32 PSU below this depth. Sampling was conducted at the edge of the ice pack in both years, and ice melt is the most likely explanation for this structure. At stn 16a, surface $[NO_3^-]$ and $[NH_4^+]$ depletion (<1 μmol L^{-1}) was observed throughout the euphotic zone in 2007. Nutrient depletion existed only in the top 20 m in 2008, with $[NO_3^-]$ increasing to ~6 μmol L^{-1} below this

depth. During both years, $[Si(OH)_4]$ in the top 20 m was up to 80% lower than concentrations below this depth. Although NPP was similar during both years (195 and 158 mg C m^{-2} d^{-1}), the 2007 f-ratio was 0.20 compared to 0.53 in 2008, and phytoplankton biomass was over 3 times higher in 2008 with a higher proportion of larger cells (86 compared to 30%). Although surface nutrient depletion was evident during both years, it is possible that the higher nutrient concentrations at the base of the euphotic zone was evidence of deep water upwelling which fueled the higher biomass seen in 2008. Silicic acid concentrations did not appear to be limiting during either year, so an abundance of NO_3^- would also account for the higher f-ratio and greater proportion of large cells observed in 2008 at this location.

At ***stns 17 and 18***, in the vicinity of the McKenzie River delta (Fig. 1.2B), nutrient concentrations in the water column were higher than elsewhere in the South Beaufort Sea, but both biomass and NPP were still low compared to other regions in the study. Stn 17 was located at the shelf break at a depth of 243 m, while stn 18 was located over the continental slope at a depth of 1000 m. Nutrient concentrations in the surface waters of the delta are determined by vertical mixing events that occurred in the previous fall and winter, and are mostly depleted by the spring bloom, following seasonal sea-ice retreat (Carmack et al., 2004). Thus, by the time of sampling in this study (mid summer, and probably post-bloom), the nutrient regime was mostly dictated by riverine inputs and upwelling events, the latter being heavily influenced by the prevailing winds, especially at stn 17 that was ice-free at the time of sampling (Environment Canada, 2011a). In the absence of heavy winds or under the influence of westerlies, riverine input from the McKenzie flows eastward and little upwelling occurs. In contrast, in the presence of

easterlies, upwelling events are common, riverine inputs move to the west and primary production is typically higher offshore (MacDonald et al., 1989). Although winds were blowing from the north at the time of sampling, they were primarily easterly during the previous month (Environment Canada, 2011b). Thus McKenzie River inputs could have been directed to the west, and upwelling favored. This was most likely the reason for the salinity difference in surface water (top ~10 m) between the two locations (24 PSU at stn 17, and 28 PSU at stn 18), and perhaps also the difference between NPP and biomass. The nutrient regimes were similar at both stations: depleted (<1 μmol L^{-1}) NO_3^- and NH_4^+ in the top 10 m of the euphotic zone, with NO_3^- increasing to ~13 μmol L^{-1} below this depth. A possible drawdown of Si was also observed as surface [$Si(OH)_4$] were somewhat lower than in deeper waters (4 μmol L^{-1} at the surface, increasing to ~28 μmol L^{-1} at the bottom of the euphotic zone).

Although both stations were probably supplied with nutrients via upwelling, stn 17 was located close to the shelf break in the vicinity of the McKenzie Canyon, leading to greater nutrient upwelling in addition to surface nutrients supplied by McKenzie River runoff. Phytoplankton activity appeared to reflect this scenario. NPP was higher at station 17 (42 compared to 32 mg C m^{-2} d^{-1} at stn 18), although f-ratios were similar (0.40 compared to 0.36). Phytoplankton biomass at stn 17 was 11.7 compared to 7.4 mg chl *a* m^{-2} at stn 18, with the assemblage being represented by a higher proportion of larger (>5 um) cells (46.3% at stn 17 compared to 21.6% at stn 18). But these were still relatively low levels of biological activity, compared to those in other regions of the present study and NPP measurements here were much lower than those quoted as the summer high (200 mg C m^{-2} d^{-1}) by Carmack et al. (2004). Taking into account these values, and that

the area was almost ice-free (10% ice cover) during this study, a reasonable assumption is that the seasonal bloom had peaked prior to sampling. The NPP values reported here were closer to those described by Carmack et al. (2004) for the later portion of the Arctic growing season (early fall), after surface nutrients are depleted by mid-summer blooms.

At ***stn 20***, sampled on the continental slope at 520 m depth, NO_3^- was depleted (<0.1 μmol L^{-1}) in the top 15 m of the water column and NH_4^+ was undetectable (<0.05 μmol L^{-1}) throughout the euphotic zone. This, and 80% ice cover were most likely the reasons for low biomass (4.9 mg chl *a* m^{-2}) at this station.

4.1.4. Canada Basin

The Canada Basin was the least variable region in terms of the physical, chemical, and biological properties. The most prominent physical feature was the 80 to 100% areal ice coverage (Environment Canada, 2011a), the exception being stn 21 which was located at the edge of the ice pack at the time of sampling.

Seawater was less saline in all stations on the top 5 to 10 m of (23 to 28 PSU) compared to the higher salinity water beneath (31 to 33 PSU), indicating ice melt and resulting in strong stratification of the water column (especially evident at stn 24, which had a surface salinity of ~16 PSU). During the summer, the melting ice may contribute a considerable amount of fresh water, overwhelming any brine release during the melting process, and thus reducing the salinity of the upper water column.

The chemical properties at all Canada Basin stations were also similar: [NO_3^-] was <1 μmol L^{-1} and at times undetectable in the top 5 to10 m of the water column below which concentrations increased to ~12 μmol L^{-1}, and NH_4^+ was almost depleted (<0.1 to 1 μmol L^{-1}) throughout the euphotic zone. Silicic acid concentrations, although more

variable, followed a similar trend as that of NO_3^-: 2 to 4 μmol L^{-1} in the top 10 m of the water column, and increasing at depth.

Phytoplankton activity seemed to reflect the expected outcome of nutrient limitation on primary production. NPP ranged from 20 to 103 mg C m^{-2} d^{-1} at the ice-covered stations, and was dominated by regenerated production at all stations (f-ratios from 0.10 to 0.37). The phytoplankton biomass was the lowest found in any region during the study (4.9 to 10.4 mg chl *a* m^{-2}) and the assemblages were dominated by smaller cells (>67%) at all stations. NPP values are consistent with those found by Lee & Whitledge (2005), who estimated an average of 40 mg C m^{-2} d^{-1} for approximately the same area sampled in this study, 2.6 to 26.8 mg C m^{-2} d^{-1} at ice-covered stations, and as high as 145 mg C m^{-2} d^{-1} at locations in open water.

4.1.5. Canadian Arctic Archipelago

Water moving through the archipelago is primarily of Pacific origin (McLaughlin et al., 2004b), and biological activity in the CAA can be viewed as the result of movement of water in one direction, with biological processes in the west impacting those farther east.

Stns 19a and 19b, in central Amundsen Gulf, were sampled on approximately the same calendar day: July 28 and July 27 in 2007 and 2008, respectively. In both years the station was ice-free but a more pronounced thermocline was evident in 2008, which may have contributed to the difference in biological activity between years. In 2007 NPP was 233 mg C m^{-2} d^{-1} and in 2008 it was 14 mg C m^{-2} d^{-1}, and f-ratios were <0.50 during both years. Although NPP was over an order of magnitude higher in 2007, phytoplankton biomass during the same year was considerably lower (14.3 compared to 82.5 mg chl *a*

m^{-2}). During both years, NO_3^- was depleted in the top 10 m of the water column, increasing to >7 μmol L^{-1} in deeper water, and NH_4^+ levels were undetectable throughout the euphotic zone. Drawdown of $Si(OH)_4$ was also evident, as [$Si(OH)_4$] was less than half of that found below this surface layer. Although N and Si depletion was evident in both years, the differences in NPP and biomass could have been attributed to the stage of the bloom at the time of sampling: 2007 could have been a mid-bloom situation, and 2008 could have been post-bloom. In 2007, NPP was higher than in 2008 and the phytoplankton biomass was low and dominated by small cells, perhaps indicative of rapid biomass turnover limiting the size of the phytoplankton standing stock. In 2008, biomass was almost 6x higher, although net C uptake was more than an order of magnitude lower than in 2007. The 2008 event may have been the end of a bloom fueled initially by upwelled NO_3^- leading to an assemblage comprised of large cells and brought to a halt by stratification of the surface layer (top 10 m) through formation of a stable thermocline by surface warming. In both cases though, NPP was primarily regenerated (f-ratio <0.50), indicating a system driven by ammonium and urea as an N source, and most likely indicating low carbon export, although the fate of the large cells observed in 2008 is uncertain.

Stn 29 was located further east in Coronation Gulf, which receives sea water moving eastwards from the Beaufort Sea via the Amundsen Gulf and fresh water inputs from the Coppermine River (Bobba et al., 2005). The structure of the water column at stn 29 suggest the influence of both water masses: the top 5 m have a salinity of ~26 PSU, and at the bottom of the euphotic zone salinity is still only 28 PSU, compared to the more saline (33 PSU) water entering from the west. This is most likely due to significant

freshwater inputs from the Coppermine River resulting in salinity values intermediate between freshwater and deep saline water. Nitrate was replete (>1 μmol L^{-1}) although NH_4^+ was undetectable throughout the euphotic zone, with the exception of the top of the water column where [NO_3^-] was ~0.5 μmol L^{-1}. NPP was 1520 mg C m^{-2} d^{-1} with an f-ratio of 0.62, and phytoplankton biomass was 24.4 mg chl *a* m^{-2} consisting primarily of larger cells (74% >5 μm). These results suggest a system driven by abundant NO_3^- supply with potentially high particle export, and possibly strong pelagic-benthic coupling due to the shallow depth (Table A1).

East of Coronation Gulf, surface waters became more saline, probably due to the diminishing influence of the Coppermine River, and more stratified, most likely due to attenuation of wind mixing in the presence of heavy (>90%) ice cover. At ***stns 30 and 31***, in Queen Maud Gulf, NO_3^- and NH_4^+ were <1 μmol L^{-1} in the top ~25 m, and $Si(OH)_4$ was more than 4 times lower than in deeper waters, suggesting active surface drawdown of N and Si by phytoplankton at both locations. Below 25 m, NO_3^- and $Si(OH)_4$ concentrations were twice as high at stn 31 compared to stn 30, possibly suggesting the presence of nutrient-rich water upwelled from the deep waters of McClintock Channel. This influx of nutrients from below the euphotic zone may have fueled primary production, and be the reason for the NPP and biomass differences between stations.

Stn 32 was located in Bellot Strait, which is a narrow and fast-flowing body of water. NO_3^- and $Si(OH)_4$ were replete at stn 32, but both biomass (6.7 mg chl *a* m^{-2}) and NPP (176 mg C m^{-2} d^{-1}) were 5 times lower than that found at stn 31. This difference was probably attributed to not only heavy (>90%) ice cover, but also an unstable water column due to turbulence.

The water column at ***stns 33 and 34***, located in Lancaster Sound, was less stratified than those stations farther west in the CAA, and it is possible that the origin of the water found at these locations was upwelled further west into the relatively shallow Barrow Strait, undergoing significant mixing in the process. Both NPP and biomass were higher at stn 33 that at stn 34, perhaps due to heavy (90%) ice cover at the latter station. Phytoplankton assemblages were mostly comprised of larger cells (88 and 75% larger) at both stations. Nitrate concentrations were <1 μmol L^{-1} in the upper water column.

4.1.6. Baffin Bay and Davis Strait

The physical and chemical properties of Baffin Bay are a result of two distinct currents. On the west side of the bay, along the Baffin Island coast, the Baffin Current is primarily a combination of Pacific origin water from Lancaster Sound and cold water moving south from Fram Strait. To the east, along the Greenland coast, the West Greenland Current moves north along the Greenland coast, meeting up with the Baffin Current at the north end of Baffin Bay.

Stns 35 and 37, along the Baffin Island east coast, were both covered by heavy ice (~90% coverage), and while being characterized by similar phytoplankton assemblages (in biomass and size), NPP was almost an order of magnitude lower at stn 37 than at stn 35 (181 compared to 1429 mg C m^{-2} d^{-1}), and the reasons for this are unclear.

Stn 38, in southern Baffin Bay, displayed the lowest biomass (4.5 mg chl *a* m^{-2}) of the Baffin Bay stations, the phytoplankton assemblage being dominated (89%) by smaller cells. NPP was also low (566 mg C m^{-2} d^{-1}), compared to the average NPP for the

region (Fig. 3.15). This may have been a result of the same factors that influence NPP at stn 37.

The nutrient regime at ***stn 39***, on the Greenland coast, is influenced primarily by the West Greenland Current; all other stations are probably primarily under the influence of polar water (Jensen et al., 1999). Stn 39 was free of ice at the time of sampling, and the water column was well mixed. During this study, NPP was 303 mg C m^{-2} d^{-1}, almost equal to the 341 mg C m^{-2} d^{-1} found by Jensen et al. (1999), but biomass was much lower (7.4 mg chl *a* m^{-2}) compared to 77.6 mg chl *a* m^{-2} measured by Jensen et al. (1999). Nitrate concentrations were > 3 µmol L^{-1} in the top 5 m of the water column, but $[Si(OH)_4]$ was <1 µmol L^{-1}, perhaps indicating Si limitation which may have brought a diatom bloom to an end before sampling. Irradiance was the highest during the cruise (average daily irradiance of 687 µeinstein m^{-2} sec^{-1}) at this station, supporting a bloom scenario, and NH_4^+ concentrations increased from nearly undetectable at the surface to ~1.3 µmol L^{-1} below 5 m, possibly indicating excretion associated with heavy grazing in the wake of a large bloom.

The high NPP (1660 mg C m^{-2} d^{-1}) found at ***stn 40*** (central Davis Strait) is possibly a product of nutrient inputs from water upwelled from the south via the West Greenland Current, and from the north as part of the mixed water moving south through Baffin Bay (Cuny et al., 2005).

4.2. Summary of Primary Production and Possible Physical and Chemical Controls in Arctic and Sub-Arctic Waters

4.2.1. Northeast Pacific Ocean

Net primary production off the coast of Vancouver Island was the highest measured during the study, the phytoplankton assemblage was comprised primarily of larger cells. These results fit with the model of a system dominated by new production, with production being driven by upwelled nutrients, and most likely exhibiting high rates of particulate organic export from surface waters. In the offshore northeast Pacific Ocean, NPP was an order of magnitude lower than that found off the coast of Vancouver Island, phytoplankton biomass and f-ratios were low, and the assemblage was comprised primarily of smaller cells. This suggests a system dominated by regenerated production, and most likely low particle export from the euphotic zone. Stations close to the Aleutian Islands, could have been influenced by a cyclonic eddy. The impact of the eddy is unclear, but both NPP and phytoplankton biomass were twice as high on the outside of the eddy, than at the center.

4.2.2. Bering and Chukchi Seas

In the southern Bering Sea, two locations were sampled: on and off the Bering Shelf. At the on-shelf station, both NPP and biomass were higher, most likely due to shelf upwelling. In the north Bering Sea variable NPP values were found, and the phytoplankton assemblage was always comprised of small cells and f-ratios were low, possibly indicating very rapid biomass turnover. In contrast, the Chukchi Sea stations were characterized by some of the highest NPP and biomass values found in the study, with assemblages comprised of primarily larger cells. The effects of seasonal ice melt has

been shown to play a significant role in the timing and magnitude of phytoplankton blooms, and locations sampled close to the edge of the ice pack had higher NPP and biomass than those to the south of the retreating ice. Stations in the vicinity of the Barrow Canyon were the most productive in the Chukchi Sea, perhaps as a result of this upwelling or ice-edge effects.

4.2.3. South Beaufort Sea

The waters off Point Barrow were surveyed in both 2007 and 2008 at the edge of the ice pack. NPP was similar in both years, but biomass was 3 times higher in 2008 and although surface nutrient depletion was evident during both years, it is possible that the higher nutrient concentrations at the base of the euphotic zone was evidence of deep water upwelling which fueled the higher biomass seen in 2008. Two locations were sampled on the McKenzie River delta: at the shelf break over the McKenzie Canyon on the western portion of the delta, and on the continental slope to the east. Nutrient regimes were mostly dictated by riverine inputs and upwelling events, the latter being heavily influenced by the prevailing winds. Local wind patterns may also have pushed McKenzie River inputs to the west, leading to the observed fresh water layer and resulting in higher NPP and biomass due to an influx of riverine nutrients.

4.2.4. Canada Basin

The Canada Basin stations were characterized by heavy ice cover, stratified surface water layer, and low near-surface nutrient concentrations. Phytoplankton activity seemed to reflect the expected outcome of nutrient limitation on primary production: NPP and biomass was the lowest found in the study and dominated by regenerated production and small cells at all stations.

4.2.5. Canadian Arctic Archipelago

The Amundsen Gulf was sampled in both 2007 and 2008. Although NPP was over an order of magnitude higher in 2007, phytoplankton biomass during the same year was 6 times lower, with differences in NPP and biomass possibly attributed to the stage of the bloom at the time of sampling: 2007 could have been a mid-bloom situation, and 2008 could have been post-bloom. In both cases NPP was primarily regenerated, most likely indicating low carbon export. The Coronation Gulf was characterized by high NPP and f-ratio and an assemblage consisting primarily of larger cells. These results suggest a system driven by abundant NO_3^- supply with potentially high particle export, and possibly strong pelagic-benthic coupling due to the shallow depth. East of the Coronation Gulf, surface waters became more saline, probably due to the diminishing influence of the Coppermine River, and more stratified, most likely due to attenuation of wind mixing in the presence of heavy ice cover. In the southern Queen Maud Gulf this most likely contributed to the observed nutrient exhaustion and low primary production. A similar water column structure existed in northern portion of the gulf, but NPP was twice as high, possibly fuelled by upwelled nutrients from the deep waters of McClintock Channel. At the east end of Bellot Strait both NPP and phytoplankton biomass were low compared to those stations in Queen Maud Gulf. This difference was possibly attributed to not only heavy (>90%) ice cover in Bellot Strait, but also a lower irradiance compared to those stations to the west. The water column in Lancaster Sound, was less stratified than those stations farther west in the CAA. The phytoplankton biomass was characterized by primarily larger cells here, possibly indicating higher organic transport to deeper water.

4.2.6. Baffin Bay and Davis Strait

Two locations were sampled along the east coast of Baffin Island. Both were covered by heavy ice, and despite being characterized by similar phytoplankton assemblages, there was an order of magnitude difference in NPP between stations, although the reasons for this are unclear. The station visited off the south Greenland coast was ice-free at the time of sampling with a well-mixed water column replete with NO_3^-., but it is possible that this resulted in Si limitation which brought a diatom bloom to an end shortly before sampling. In Davis Strait, NPP was high and likely a product of nutrient inputs from water upwelled from the south via the West Greenland Current, and from the north as part of the mixed water moving south through Baffin Bay.

4.3. Revisiting the Thesis Objectives

Characterization of the structure of the phytoplankton community and Determination of primary productivity

All parameters measured in this thesis were found to be highest in the Bering and Chukchi Seas; all parameters were found lowest in the Canada Basin (Table 4.1). The possible physical and chemical controls behind these results are discussed in section 4.2.

Table 4.1. Regional means of measured biological parameters. Variability is presented as standard error.

Region	**Phytoplankton Biomass (mg chl *a* m^{-2})**	**Cells >5 µm (%)**	**Net Primary Production (mg C m^{-2} d^{-1})**	**f-ratio**
Northeast Pacific Ocean	16.8±3.8	27.9±4.5	393.7±134.7	0.48±0.15
Bering & Chukchi Seas	39.2±9.6	68.1±9.8	997.8±230.6	0.57±0.12
South Beaufort Sea	13.4±4.7	38.9±13.1	89.3±36.2	0.32±0.07
Canada Basin	7.6±0.7	19.7±2.3	54.4±8.4	0.24±0.07
Canadian Arctic Archipelago	25.8±8.6	66.5±5.8	540.2±171.0	0.39±0.08
Baffin Bay & Davis Strait	25.0±9.6	51.8±12.7	992.6±296.3	0.35±0.05

Test the validity of the regional and shelf-type classification scheme

The regional classification scheme employed to divide the study area into discrete regions proved to be an appropriate method of creating geographic divisions between regions with dissimilar biological properties. Although the mean values of several of the parameters are similar (e.g. NPP in the Bering & Chukchi Seas compared to Baffin Bay & Davis Strait), there were still noticeable differences in parameter means between geographically adjacent regions, especially in regards to NPP and Phytoplankton Biomass, further reinforcing the validity of regional division.

Examine the relationship between measured biological and physical parameters

The concept of bottom-up control was introduced as the overlying reason for the trends in phytoplankton production found during this study, and in most cases this concept held true. NPP and phytoplankton biomass increased concurrently throughout the study area (Fig. 4.1A), governed by the same basic chemical and physical controls, although each region was different in regards to specific controls (such as nutrient availability or ice cover) as discussed in sections 4.1 and summarized in section 4.2.

4.4. Regional Export Production and Biological Pump

Eppley & Peterson (1979) suggested that a high proportion of new production, often characterized by a phytoplankton biomass comprised of primarily larger cells, tends to be indicative of high C export to deeper waters. Therefore, high f-ratios and a high biomass of cells >5 μm may be indicators of high particulate export from surface waters; a correlation coefficient of 0.426 (Figure 4.1B) supports this relationship for the pan-Arctic stations covered during this study.

Phytoplankton biomass was not significantly different between regions, but only marginally so ($p = 0.057$; Table 3.1) and NPP was significantly different ($p = 0.000$) with a wide range of f-ratios, indicating differences from region-to-region in the magnitude of the biological pump and resulting particulate export from surface waters. Region 1 (Northeast Pacific Ocean), as defined in this thesis, was comprised mostly of offshore stations with a moderately high NPP and f-ratio (Fig. 3.15). Although the single station off the coast of Vancouver Island offered the potential for high particulate export, the region as a whole, being mostly offshore, was probably characterized by low overall

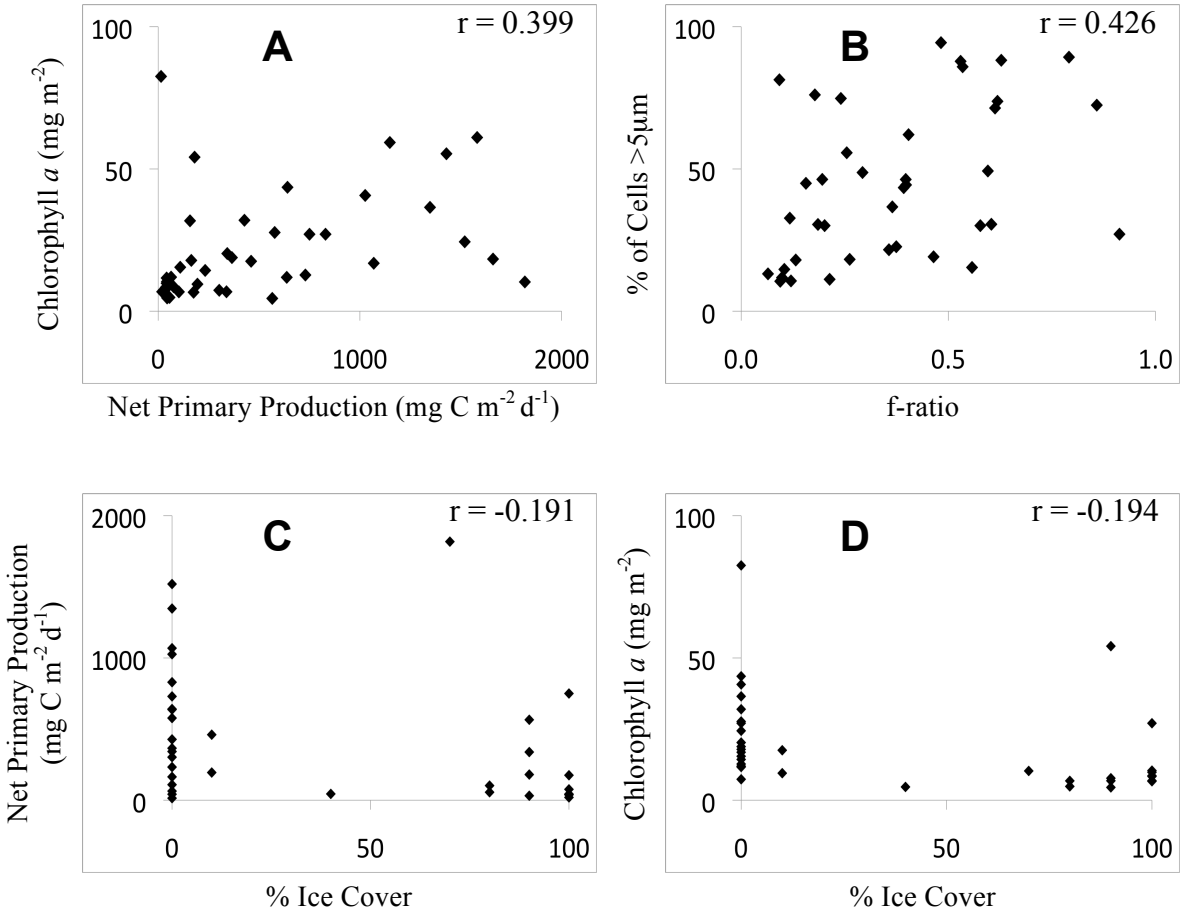

Figure 4.1. Correlation plots for A: total chlorophyll *a* and NPP; B: percent of biomass for cells >5 µm; C: NPP and ice cover; and D: total chlorophyll *a* and ice cover. Correlation coefficients (Pearson coefficient) are shown in the top-right corner of each plot.

export, as previously found by Varela and Harrison (1999) and Peña and Varela (2007). Region 2 (The Bering and Chukchi Seas) had the highest NPP and f-ratio in the pan-Arctic study area, suggesting high particulate export. Unlike the Pacific Ocean, the relatively shallow depth may complicate the biological pump mechanism introduced in section 1.1.2, but nevertheless the potential for significant removal of carbon from surface waters is possible in this region, especially in the Chukchi Sea. In both, Regions 3 and 4 (South Beaufort Sea and Canada Basin) NPP was relatively low compared to the other region, and f-ratios were <0.50, indicating a system based on regenerated production and exhibiting low particulate export. Regions 5 and 6 (Canadian Arctic Archipelago and Baffin Bay/Davis Strait), although variable with regards to NPP, both exhibited f-ratios >0.50, and the possibility of significant particulate export.

4.5. Possible Effects of Global Warming on Arctic Primary Production

The most noticeable effect of global warming in the Arctic Ocean is the pronounced reduction in sea ice cover compared to historical norms. In most of the regions sampled, ice cover or the lack thereof played a significant role in influencing primary production (Fig. 4.1C and 4.1D). In the Canada Basin the presence of heavy sea ice resulted in low primary production due to irradiance attenuation and the prevention of wind-driven vertical mixing. Temporary water column stabilization in the wake retreating seasonal ice appeared to have a considerable role in increasing primary production through removal of irradiance attenuation and temporary stratification of the water column in the presence of high nutrient load from the previous winter.

More persistent stratification could have the opposite effect. In addition to a marked reduction in surface salinity, a persistently stratified water column could reduce

wind-driven nutrient upwelling, thus reducing primary production. This phenomenon could be most noticeable in the Canada Basin where meltwater may continue to be a factor for years to come, and the circulation of the Beaufort Gyre may keep surface melt water trapped in the area for some time even after all sea ice has melted.

Global warming could increase stratification through terrestrial inputs as well. A higher volume of freshwater inputs from the McKenzie or Yukon Rivers due to increasing snowpack melt could significantly increase surface stratification in the north Bering and South Beaufort Seas, with the effects on primary production noted above. In Baffin Bay, runoff from a quickly melting Greenland icepack could result in the same effect, as would glacial runoff throughout the Canadian Arctic Archipelago.

Whatever the effect of increasing sea ice melt on to the structure of the water column may be, a reduction of sea ice volume may effectively increase the growing season in the Arctic by removing PAR limitation. This phenomenon, in conjunction with increased wind-driven upwelling events that bring nutrients into the euphotic zone, could lead to increased primary production in previously unproductive ice covered areas.

4.6. Future Research Directions

The most critical component regarding sampling design in the Arctic is timing. As mentioned above, the edge of the seasonal ice pack is a dynamic front with regards to primary production and blooms occurring there appear to be brief in nature. Designing a research programme that followed the receding ice north would be instrumental in determining the potential for carbon export in the Arctic, especially in extremely productive areas like the south Chukchi Sea, Barrow Canyon area or in the largely undersampled Canadian Arctic Archipelago.

Due to the large spatial and temporal variations that result from sequentially sampling a geographically vast study area, it would be ideal for simultaneous data collection at a variety of locations. This is clearly impossible considering the experimental approach taken in this study. Remote sensing, by using ocean colour as a proxy for phytoplankton biomass, can offer a solution to the spatial and temporal issues. At present, the presence of sea ice makes the remote sensing approach quite impractical and we still require *in situ* data collection such as that conducted in this thesis project. But improved technology in conjunction with potentially rapid sea ice melting may improve the feasibility of a remote sensing approach, although it is still critical to conduct in situ data collection to ground-truth the remote sensing estimates.

This project represented a unique opportunity to build on the conclusions of previous studies while significantly adding new data to the limited body of knowledge on phytoplankton dynamics in sub-Arctic and Arctic marine waters. The study presented in this thesis is valuable as a standalone project, offering a snapshot of phytoplankton dynamics during 2007 and 2008, but also providing important baseline data for future studies of phytoplankton dynamics in this diverse and rapidly changing region.

4.7. Summary of Major Project Results and Recommendations

- The highest primary production and phytoplankton biomass values were observed in the Bering and Chukchi Seas.
- The lowest primary production and phytoplankton biomass values were observed in the Canada Basin.
- Future studies should focus on biological ‘hot spots’ (eg. Barrow Canyon) and undersampled regions (eg. The Canadian Arctic Archipelago).

- Future studies should take into account the often brief nature of phytoplankton blooms - especially at the ice edge – by incorporating time series observations into the research methodology.

REFERENCES

Aagaard, K. (1984). The Beaufort undercurrent. In Barnes, P., & Reimnitz, E. (Eds.), *The Alaskan Beaufort Sea: Ecosystems and environment*, pp. 47-71. New York: Academic Press.

Alexander, V., & Niebauer, H. J. (1981). Oceanography of the eastern Bering Sea ice-edge zone in spring. *Limnology and Oceanography*, 26, 1111-1125.

Andersen, O. G. N. (1981). The annual cycle of phytoplankton primary production and hydrography in the Disco Bugt area, West Greenland. *Meddelelser om Grønland Bioscience*, 6, 1–68.

Anderson, O. G. N. (1989). Primary production, chlorophyll, light, and nutrients beneath the Arctic sea ice. In Herman, Y. (Ed.), *The Arctic seas. Climatology, oceanography, geology, and biology*, pp. 147-191. New York: Van Nostrand Reinhold.

Arrigo, K. R., & van Dijken, G. L. (2004). Annual cycles of sea ice and phytoplankton in Cape Bathurst polynya, southeastern Beaufort Sea, Canadian Arctic. *Geophysical Research Letters*, 31, L08304. doi: 10.1029/2003GL018978

Arrigo, K. R., van Dijken, G. L., & Pabi, S. (2008). Impact of a shrinking Arctic ice cover on marine primary production, *Geophysical Research Letters*, 35, L19603. doi:10.1029/2008GL035028.

Bailey, W. B. (1957). Oceanographic features of the Candian Arctic Archipelago. *Journal of the Fisheries Research Board of Canada*, 14, 731-769.

Bates, N. R., Best, M. H. P., & Hansell, D. A. (2005). Seasonal and spatial distribution of particulate organic matter (POM) in the Chukchi and Beaufort Seas. *Deep Sea Research II*, 52, 3324-3343.

Bobba, A. G., Prowse, T. D., Diiwu, J. Y., & Milburn, D. (2005). Sensitivity of hydrological variables in the Arctic watershed, Coppermine River, NWT, Canada due to hypothetical climate change. *Journal of Environmental Hydrology*, 13, paper 22.

Boyd, P., & Harrison, P. J. (1999). Phytoplankton dynamics in the NE subarctic Pacific. *Deep-Sea Research II*, 46, 2405-2432.

Boyd, P. W., Law, C. S., Wong, C.S., Nojiri, Y., Tsuda, A., Levasseur, M., Takeda, S., Rivkin, R., Harrison, P. J., Strzepek, R., Gower, J., Mckay, R. M., Abraham, E., Arychuk, M., Barwell-Clarke, J., Crawford, W., Crawford, D., Hale, M., Harada, K., Johnson, K., Kiyosawa, H., Kudo, I., Marchetti, A., Miller, W., Needoba, J.,

Nishioka, J., Ogawa, H., Page, J., Robert, M., Saito, H., Sastri, A., Sherry, N., Soutar, T., Sutherland, N., Taira, Y., Whitney, F., Wong, S. E., & Yoshimua, T. (2004). The decline and fate of an iron-induced subarctic phytoplankton bloom. *Nature*, 428, 549-553.

Brugel, S., Nozais, C., Poulin, M., Tremblay, J., Miller, L. A., Simpson, K. G., Gratton, Y., & Demers, S. (2009). Phytoplankton biomass and production in the southeastern Beaufort Sea in autumn 2002 and 2003. *Marine Ecology Progress Series*, 377, 63-77.

Brzezinski, M. A., & Nelson, D. M. (1986). A solvent extraction method for the colorimetric determination of nanomolar concentrations of silicic water in seawater. *Marine Chemistry*, 19, 139-151.

Carmack. E. C., & Macdonald, R. W. (2002). Oceanography of the Canadian Shelf of the Beaufort Sea: A setting for marine life. *Arctic*, 56(1), 29-45.

Carmack, E. C., & Chapman, D. C. (2003). Wind-driven shelf/basin exchange on an Arctic shelf: The joint roles of ice cover extent and shelf-break bathymetry. *Geophysical Research Letters*, 30, 1778. doi: 10.1029/2003GL017526

Carmack, E. C., Macdonald, R. W., & Jasper, S. (2004). Phytoplankton productivity on the Canadian Shelf of the Beaufort Sea. *Marine Ecology Progress Series*, 277, 37-50.

Carmack, E. C., & Wassmann, P. (2006). Food webs and physical-biological coupling on pan-Arctic shelves: Unifying concepts and comprehensive perspectives. *Progress in Oceanography*, 71, 446-477.

Carmack, E. C., McLaughlin, F., Vagle, S., & Melling, H. (2008). Canada's Three Oceans (C3O): A Canadian contribution to the International Polar Year. *PICES Press*, 16, 22-25.

Carmack, E. C. & McLaughlin, F. (2011). Towards recognition of physical and geochemical change in Subarctic and Arctic Seas. *Progress In Oceanography*, 90, 90-104.

Cota, G. F., Pomeroy, L. R, Harrison, W. G., Jones, E. P., Peters, F., Sheldon, W. M., & Weingartner, T. R. (1996). Nutrients, primary production and microbial heterotrophy in the southeastern Chukchi Sea: Arctic summer nutrient depletion and heterotrophy. *Marine Ecology Progress Series*, 135, 247-258.

Cuny, J., Rhines, P. B., & Kwok, R. (2005). Davis Strait volume, freshwater and heat fluxes. *Deep Sea Research Part I: Oceanographic Research Papers*, 52, 519-542.

Dickson, A. G., & Goyet, C. (Eds.). (1994). *Handbook of methods for the analysis of the various parameters of the carbon dioxide system in sea water, Rep. ORNL/CDIAC-74*. Washington: U.S. Department of Energy.

Dugdale, R. C., & Goering, J. J. (1967). Uptake of new and regenerated nitrogen in primary productivity. *Limnology and Oceanography*, 12, 196-206.

Dugdale, R. C., & Wilkerson, F. (1986). The use of ^{15}N to measure nitrogen uptake in eutrophic oceans; experimental considerations. *Limnology and Oceanography*, 31, 673-689.

Dugdale, R. C., & Wilkerson, F. (1991). Low specific nitrate uptake rate: A common feature of high-nutrient, low-chlorophyll marine ecosystems. *Limnology and Oceanography*, 36, 1678-1688.

Dunbar, M.J. (1982). Arctic marine ecosystems. In Rey, L. (Ed.), *The Arctic Ocean*, pp. 233-252. Monaco: Comite Arctique.

English, T. S. (1961). Some biological oceanographic observations in the central north polar sea. Drift Station Alpha, 1957-1958. *Arctic Institute of North America Research Papers*, 13, viii-80.

Environment Canada. *Canadian ice service, latest ice conditions*. (2011a, April). Retrieved from http://www.ec.gc.ca/glaces-ice

Environment Canada. *Canada's national climate archive*. (2011b, April). Retrieved from http://www.climate.weatheroffice.gc.ca

Eppley, R., & Peterson, B. J. (1979). Particulate organic matter flux and planktonic new production in the deep ocean. *Nature*, 282, 677-680.

Falkowski, P. G., & Raven, J. A. (2007). *Aquatic Photosynthesis (2nd edition)*. Princeton, New Jersey: Princeton University Press.

Field, C., Behrenfeld, M., Randerson, J., & Falkowski, P. (1998) Primary prodiction of the biosphere: Integrating terrestrial and oceanic components. *Science*, 281, 237-240.

Gao, Y., Kaufman, Y. J., Tanré, D., Kolber, D., & Falkowski, P. G. (2001), Seasonal distributions of aeolian iron fluxes to the global ocean. *Geophysical Research Letters*, 28, 29-32.

Gosselin, M., LeVasseur, M., Wheeler, P. A., Horner, R. A., & Booth, B. C. (1997). New measurements of phytoplankton and ice algal production in the Arctic Ocean. *Deep-Sea Research II,* 44, 1623-1644.

Grebmeier, J. M., & Barry, J. P. (1991). The influence of oceanographic processes on pelagic-benthic coupling in polar regions: a benthic perspective. *Journal of Marine Systems*, 2, 495-518.

Grebmeier, J., Cooper, L., Feder, H., & Sirenko, B. (2006). Ecosystem dynamics of the Pacific-influenced Northern Bering and Chukchi Seas in the Amerasian Arctic. *Progress in Oceanography*, 71, 331-361.

Hama, T., Miyazaki, T., Ogawa, Y., Iwakuma , T., Takahashi, M., Otsuki, A., & Ichimura, S. (1983). Measurement of photosynthetic production of a marine phytoplankton population using a stable ^{13}C isotope. *Marine Biology*, 73, 31-36.

Hansell, D.A., Whitledge, T.E., & Goering, J.J. (1993). Patterns of nitrate utilization and new production over the Bering–Chukchi shelf. *Continental Shelf Research*, 13, 601–627.

Harrison, W. G., & Cota. G. F. (1991). Primary production in polar waters: relation to nutrient availability. In Sakashaug, E., Hopkins, C. C. E., & Oritsland, N. A. (Eds.), *Proceedings of the Pro Mare Symposium on Polar Marine Ecology. Trondheim. 12-16 May 1990*, pp 87-104. Polar Research 1O(1).

Harrison, P. J., Boyd, P. W., Varela, D. E., Takeda, S., Shiomoto, A., & Odate, T. (1999). Comparison of factors controlling phytoplankton productivity in the NE and NW subarctic Pacific gyres. *Progress in Oceanography*, 43, 205–234

Hill, V., & Cota, G. (2005). Spatial patterns of primary production on the shelf, slope and basin of the Western arctic in 2002. *Deep-Sea Research II*, 52, 3344-3354.

Holmes, R. M., Aminot, A., Kerouel, R., Hooker, B. A., & Peterson, B. J. (1999). A simple and precise method for measuring ammonium in marine and freshwater ecosystems. *Canadian Journal of Fisheries and Aquatic Sciences*, 56, 1801-1808.

Hunt, G. L., Stabeno, P., Walters, G., Sinclair, E., Brodeur, R. D., Napp, J. M., Bond, N. A. (2002) Climate change and control of the southeastern Bering Sea pelagic ecosystem. *Deep-Sea Research*, 49, 5821–5853.

Ingram, R., Bacle, J., Barber, D., Gratton, Y., & Melling, H. (2002). An overview of physical processes in the North Water. *Deep-Sea Research Part II-Topical Studies In Oceanography,* 49, 4893-4906.

IPCC (Intergovernmental Panel on Climate Change). (2001). The Core Writing Team Synthesis Report. In Watson, R. T. (Ed.), *IPCC Third Assessment Report, Climate Change 2001*. Geneva, Switzerland

Jensen, H. M., Pedersen, L., Burmeister, A., & Hansen, B. W. (1999). Pelagic primary production during summer along 65 to 72^{o}N off West Greenland. *Polar Biology*,

21, 269-278. Jones, E. P., & Coote, A. R. (1980). Nutrient distributions in the Canadian Archipelago: Indicators of summer water mass and flow characteristics. *Canadian Journal of Fisheries and Aquatic Sciences*, 37, 589-599. doi: 10.1139/f80-075

Jones, E. P., Swift, J. H., Anderson, L. G., Lipizer, M., Civitarese, G., Falkner, K. K., Kattner, G., & McLaughlin, F. (2003). Tracing Pacific water in the North Atlantic Ocean. *Journal of Geophysical Research*, 108, 3116. doi:10.1029/2001JC001141

Kostianoy A. G., Nihoul J. C. J. & Rodionov V. B. (2004). *Physical oceanography of the frontal zones in sub-Arctic seas*. Elsevier: Elsevier Oceanography Series.

Lalli, C. M., & Parsons, T. R. (1993). *Biological oceanography, an introduction (2nd edition)*. Oxford: Butterworth-Heinemann.

Lavoie, D., Denman, K. L., & Macdonald, R.W. (2009). Primary productivity and export fluxes on the Canadian shelf of the Beaufort Sea: a modelling study. *Journal of Marine Systems*. 75, 17-32.

Lovvorn, J. R., Cooper, L. W., Brooks, M. L., De Ruyck, C. C., Bump, J. K., & Grebmeier, J. M. (2005). Organic matter pathways to zooplankton and benthos under pack ice in late winter and open water in late summer in the north-central Bering Sea. *Marine Ecology Progress Series*, 291, 135-150.

Lee, S. H., & Whitledge, T. E. (2005). Primary and new production in the deep Canada Basin during summer 2002. *Polar Biology*, 28, 190-197.

Lee, S. H., Whitledge, T. E., & Kang, S. (2007). Recent carbon and nitrogen uptake rates of phytoplankton in Bering Strait and the Chukchi Sea. *Continental Shelf Research*, 27, 2231-2249.

Legendre, L., & Gosselin, M. (1996). Estimation of N and C uptake rates by phytoplankton using ^{15}N and ^{13}C: revisiting the usual computational formulae. *Journal of Plankton Research*, 19, 263-271.

Macdonald, R.W., Carmack, E. C., McLaughlin, F. A., Iseki, K., Macdonald, D. M., & O'Brien, M. C. (1989). Composition and modification of water masses in the Mackenzie Shelf Estuary. *Journal of Geophysical Research*, 94, 18,057-18,070.

Macdonald, R. W., Solomon, S. M., Cranston, R. E., Welch, H. E., Yunker, M. B., & Gobeil, C. (1998). *A sediment and organic carbon budget* for the Canadian Beaufort Shelf. *Marine Geology*, 144, 255–273.

Martin, J. H., & Fitzwater, S. (1988). Iron deficiency limits phytoplankton growth in the north-east Pacific subarctic. *Nature*, 331, 341-343

Mathews, J. B. (1981). Observations of surface and bottom currents in the Beaufort Sea Near Prudhoe Bay, Alaska. *Journal of Geophysical Research*, 86, 6653-6660.

McLaughlin, F. A., Carmack, E. C., Macdonald, R., & Bishop, J. (1996). Physical and geochemical properties across the Atlantic/Pacific water mass boundary in the southern Canadian Basin. *Journal of Geophysical Research*, 101, 1193-1198.

McLaughlin, F. A., Carmack, E. C., Macdonald, R. W., Melling, H., Swift, J. H., Wheeler, P. A., Sherr, B. F., & Sherr, E. B. (2004a). The joint roles of Pacific and Atlantic-origin waters in the Canada Basin, 1997–1998. *Deep Sea Research I*, 51, 107-128.

McLaughlin, F. A., Carmack, E. C., Ingram, R. G., Williams, W., & Michel, C. (2004b). Oceanography of the Northwest Passage. In Robinson, A. R., & Brink, K. H. (Eds.), *The sea, vol. 14*, pp. 1211-1242. Cambridge: Harvard University Press.

McRoy, C. P., Goering, J. J., & Shiels, W. E. (1972) Studies of primary production in the eastern Bering Sea. In Takenouti, A. Y. (Ed.), *Biological Oceanography of the North Pacific Ocean*, pp. 199–216. Tokyo: Idemitsu-shoten.

McRoy, C. P. (1993). ISHTAR, the project: an overview of the inner shelf transfer and recycling in the Bering and Chukchi seas. *Continental Shelf Research*, 13, 473-479.

Michel, C., Ingram, R. G., & Harris, L. R. (2006). Variability in oceanographic and ecological processes in the Canadian Arctic Archipelago. *Progress in Oceanography*, 71, 379-401.

Mordy, C. W., Stabeno, P. J., Ladd, C., Zeeman, S., Wisegarver, D. P., Salo, S. A., & Hunt, G. L. (2005). Nutrients and primary production along the eastern Aleutian Island Archipelago. *Fisheries Oceanography*, 14, 55-76.

Mulvenna, P. F., & Savidge, G. (1992). A modified manual method for the determination of urea in seawater using diacetylmonoxime reagent. *Estuarine, Coastal and Shelf Science*, 34, 429-438.

Nielsen, T. G., & Hansen, B. W. (1999). Phytoplankton community structure and carbon cycling in the western coast of Greenland during the stratified summer situation. I. Hydrography, phytoplankton and bacterioplankton. *Aquatic Microbial Ecology*, 16, 205-216.

Omstedt, A., Carmack, E. C., & Macdonald, R. (1994). Modelling the seasonal cycle of salinity in the Mackenzie shelf/estuary. *Journal of Geophysical Research*, 99, 10,011-10,021.

Parsons, T. R., Maita, Y., & Lalli, C. M. (1984). *A manual of biological and chemical methods for seawater analysis*. Oxford: Pergamon Press.

Peña, M. A., & Varela, D. E. (2007). Seasonal and interannual variability in phytoplankton and nutrient dynamics along Line P in the NE subarctic Pacific. *Progress in Oceanography*, 75, 200-222.

Perovich, D. K., Light, B., Eicken, H., Jones, K. F., Runciman, K., & Nghiem, S. V. (2007). Increasing solar heating of the Arctic Ocean and adjacent seas, 1979–2005: Attribution and role in the ice-albedo feedback. *Geophysical Research Letters*, 34, L19505. doi:10.1029/2007GL031480

Reynolds, C. (2006). *Ecology of Phytoplankton*. Cambridge: Cambridge Press.

Sakshaug, E. (2004). Primary and secondary production in the Arctic seas. In Stein, R., & Macdonald, R.W. (Eds.), *The organic carbon cycle in the Arctic Ocean*, pp. 57-81. New York: Springer.

Sorteberg, A., Furevik, T., Drange, H., & Kvamsto, N. G. (2005). Effects of simulated natural variability on Arctic temperature projections. *Geophysical Research Letters*, 32, L18708.

Smith, R. E. H., Anning, J. H., Clement, P., & Cota, G. F. (1988). Abundance and production of ice algae in Resolute Passage, Canadian Arctic. *Marine Ecology Progress Series*, 48, 251-263.

Smith, W. O, & Nelson, D. M. (1985). Phytoplankton bloom produced by a receding ice edge in the Ross Sea: Spatial coherence with the density field. *Science*, 227, 163-166.

Spence, C., & Burke, A. (2008). Estimates of Canadian Arctic Archipelago runoff from observed hydrometric data. *Journal of Hydrology*, 362, 247-259.

Springer, A. M., & McRoy, C. P. (1993). The paradox of pelagic food webs in the northern Bering Sea III. Patterns of primary productivity. *Continental Shelf Research*, 13, 575-599.

Stabeno, P. J., Hunt, G. L., Napp, J. M., & J. D. Schumacher, J. D. (2006). Physical forcing of ecosystem dynamics on the Bering Sea Shelf. In Robinson, A. R., & Brink, K. (Eds.), *The sea, vol. 14*, 1177-1212. Cambridge: Harvard University Press.

Stabeno, P. J., Ladd, C., & Reed, R. K. (2009). Observations of the Aleutian North Slope Current, Bering Sea, 1996-2001. *Journal of Geophysical Research*, 114, C05015.

Strickland, J. D. H., & Parsons, T. (1972). *A practical handbook of seawater analysis, 2nd edition*. Ottawa: Fisheries Research Board of Canada.

Syrett, P. J. (1981). Nitrogen metabolism of microalgae. In Trevor Platt (Ed.), *Physiological Bases of Phytoplankton Ecology*, p. 182. Ottawa: Dept of Fisheries and Oceans Canada Bulletin 210.

Thomson, D. H. (1982). Marine benthos in the eastern Canadian high arctic: multivariate analyses of standing crop and community structure. *Arctic*, 35, 61-74.

Tsuda, A., Takeda, S., Saito, H., Nishioka, J., Nojiri, Y., Kudo, I., Kiyosawa, H., Shiomoto, A., Imai, K., Ono, T., Shimamoto, A., Tsumune, D., Yoshimura, T., Aono, T., Hinuma, A., Kinugasa, M., Suzuki, K., Sohrin, Y., Noiri, Y., Tani, H., Deguchi, Y., Tsurushima, N., Ogawa, H., Fukami, K., Kuma, K., Saino, T. (2003). A mesoscale iron enrichment in the western subarctic Pacific induces a large centric diatom bloom. *Science*, 300, 958-961.

Varela, D. E., & Harrison, P. J. (1999). Seasonal variability in nitrogenous nutrition of phytoplankton assemblages in the northeastern subarctic Pacific Ocean. *Deep-Sea Research II*, 46, 2505-2538

Walsh, J. J., McRoy, C. P., Coachman, L. K., Goering, J. J., Nihoul, J. J., Whitledge, T. E., Blackburn, T. H., Parker, P. L., Wrick, C. D., Shuert, P. G., Grebmeier, J. M., Springer, A. M., Tripp, R. D., Hansell, D. A., Djenidi, S., Deleersnuder, E., Henriksen, K., Lund, B. A., Andersen, P., Muller-Karger, F. E., & Dean, K. (1989). Carbon and nitrogen cycling within the Bering/Chukchi Seas: Source regions for organic matter effecting AOU demands of the Arctic Ocean. *Progress in Oceanography*, 22, 277-339.

Wang, J., Cota, G. F., & Comiso, J. C. (2005). Phytoplankton in the Beaufort and Chukchi seas: distribution, dynamics, and environmental forcing. *Deep-Sea Research II*, 52, 3355–3368.

Ward, B. B. (1986). Nitrification in marine environments. In Prosser, J. I. (Ed.), *Nitrification*, *Special publications of the Society for General Microbiology, vol. 20*., pp. 117-126. Oxford: IRL Pres.

Welch, H. E., & Kalff, J. (1975). Marine metabolism at Resolute Bay, Northwest Territories. In *Proceedings of the Circumpolar Conference on Northern Ecology, Part II*, pp. 67-75. Ottawa: NRC Canada.

Welch, H. E., Bergmann, M. A., Siferd, T. D., Martin, K. A., Curtis, M. F., Crawford, R. E., Conover, R. J., & Hop, H. (1992). Energy flow through the marine ecosystem of the Lancaster Sound region, Arctic Canada. *Arctic*, 45, 343-357.

Woods Hole Oceanographic Institution. *Beaufort Gyre Circulation*. (2010, April). Retrieved from http://www.whoi.edu/beaufortgyre/results_bgcirculation.html

Wilkinson, T. A. C., Wiken, E., Creel, J. B., Hourigan, T. F., Agardy, T., Herrmann, H., Janishevski, L., Madden, C., Morgan, L., and Padilla, M. (2009). *Marine ecoregions of North America*. Montreal: Commission on Environmental Cooperation.

Woodgate, R. A., Aagaard, K., & Weingartner, T. (2005). A Year in the physical oceanography of the Chukchi Sea: moored measurements from autumn 1990-1991. *Deep-Sea Research*, 52, 3116–3149.

Wyatt, S. N. (2010). A pan-Arctic perspective on the contribution of siliceous phytoplankton to autotrophic biomass in Canada's Oceans. Honours Thesis, Department of Biology, University of Victoria, Victoria. Canada. 68 pp.

APPENDIX A. SAMPLING LOCATIONS AND PHYSICAL FEATURES

Table A.1. Physical features of stations sampled in this thesis. Note that stations 16a and 16b are labelled in the opposite order to those stations in Wyatt (2010).

Station Number (in thesis)	Sampling Date	C3O Station Name	Latitude (^{o}N)	Longitude (^{o}W)	Bottom Depth (m)	Euphotic Zone Depth (m)	Ice Cover (%)
1	July 3, 2008	NP-1	49.1191	126.6906	136	79	0
2	July 5, 2008	NP-5	51.6447	136.6593	3641	100	0
3	July 6, 2008	NP-6	53.4888	139.7616	3562	71	0
4	July 7, 2008	NP-8	52.6196	142.4761	3862	119	0
5	July 8, 2008	NP-9	53.0954	148.0521	4263	70	0
6	July 10, 2008	NP-12	53.7120	156.1248	4718	102	0
7	July 10, 2008	NP-13	53.7021	159.2917	6900	80	0
8	July 11, 2008	NP-14	53.7433	161.1096	3999	100	0
9	July 15, 2008	BCL-2	55.0607	170.2157	2441	100	0
10	July 14, 2008	BS-5	56.6520	172.7348	134	50	0
11	July 16, 2008	SLIP-4	63.0263	173.4562	74	59	0
12	July 17, 2008	UTBS-1	64.9902	169.1402	49	44	0
13	July 19, 2008	UTN-4	67.5041	168.9026	51	42	0
14	July 20, 2008	CCL-4	69.9910	168.0202	495	30	60 ice edge
15	July 21, 2008	BC-2	71.4137	157.4971	127	44	70 ice edge
16a	August 3, 2007	BL-2	71.4017	152.0473	160	49	10
16b	July 23, 2008	BL-1	71.3241	152.2125	63	59	20 ice edge
17	July 25, 2008	MK-1	70.2298	140.0039	243	97	0
18	July 26, 2008	BFB-5	71.3332	133.7479	1000	90	80 ice edge
19a	July 28, 2007	AG-5	70.5472	122.8975	640	85	0
19b	July 27, 2008	BFB-7	70.5447	122.5447	665	60	0
20	July 30, 2007	BI-2	73.8238	129.1987	520	132	80
21	July 31, 2007	CB-29	71.9917	140.0398	2685	159	80
22	August 4, 2007	CB-2a	72.4992	150.0450	2690	65	100
23	August 6, 2007	CB-4	74.9203	150.1472	3830	70	100
24	August 7, 2007	RS-1	75.7468	157.0967	991	92	40
25	August 9, 2007	CB-9	77.9348	149.8262	1488	79	100
26	August 12, 2007	CB-11b	79.9885	150.0118	3820	95	100
27	August 14, 2007	CB-15	76.9990	140.1874	3734	99	100
28	August 23, 2007	CB-21	73.9670	140.0880	3502	106	90
29	July 25, 2007	CAA-16	68.3820	113.1139	216	57	0
30	July 24, 2007	CAA-12	68.6729	103.9165	103	55	90
31	July 23, 2007	CAA-10	70.6507	98.5886	193	50	100
32	July 22, 2007	CAA-6	71.9487	94.2889	82	70	100

33	July 20, 2007	CAA-5	73.5254	89.5113	434	54	0
34	July 17, 2007	CAA-2	74.2182	85.6458	556	50	10
35	July 16, 2007	BEW-11	72.3847	73.8941	152	70	100 fast ice
36	July 14, 2007	BB-10	71.5659	65.4011	2300	70	70
37	July 12, 2007	BB-8	68.0852	64.0060	156	60	90
38	July 12, 2007	BB-5	68.8308	61.7605	1800	65	90
39	July 11, 2007	BB-1	69.1953	56.4217	244	80	0
40	July 10, 2007	LS-7	66.0000	57.6730	590	50	30 ice edge
41	July 8, 2007	LS-4	58.4890	53.6622	3382	60	0
42	July 7, 2007	LS-2/Stn-2	54.2531	54.1001	217	50	0

Table A.2. Physical features of stations sampled as part of the C3O project, but not referenced in this thesis.

C3O Station ID	Sampling Date	Latitude (^{o}N)	Longitude (^{o}W)	Sampling Depth (m)	Bottom Depth (m)
UN-7	July 11, 2008	53.7336	163.9314	6	1343
UN-4	July 11, 2008	53.9598	164.3328	3	109
UN-2	July 11, 2008	54.1115	164.5808	3	89
BS-1	July 14, 2008	56.3145	172.8167	3	3000
BS-3	July 14, 2008	56.4773	172.7805	3	835
BCL-6	July 17, 2008	63.9982	171.9908	3	54
BC-4	July 22, 2008	71.9330	154.8923	6	582
BFB-6	July 26, 2008	70.8262	127.4236	6	182
BL-4	August 4, 2007	71.5023	151.6572	5	1012
BL-1	August 3, 2007	71.3250	152.2176	5	60
CB28aa	August 2, 1978	70.0032	140.0098	2	58
MK-1	August 1, 2007	70.2298	140.0042	2	220
MK-3	August 1, 2007	70.5821	140.0484	1	824
BE-2	July 28, 2007	72.0060	94.5858	15	69

APPENDIX B. PHYTOPLANKTON PRODUCTION AND BIOMASS DATA

Table B.1. Biological properties (integrated) of stations sampled as part of this thesis. Note that stations 16a and 16b are labelled in the opposite order to those stations in Wyatt (2010).

Station Number (in thesis)	Net Primary Production (mg C m^{-2} d^{-1})	f-ratio	Total Biomass (mg chl a m^{-2})	Biomass >5 μm (%)
1	6182	NO DATA	51.8	71
2	109	0.91	15.5	27
3	64	NO DATA	12.0	19
4	638	0.39	11.9	43
5	428	0.46	32.0	19
6	730	0.19	12.7	31
7	1348	0.58	36.5	30
8	578	0.06	27.7	13
9	366	NO DATA	18.9	14
10	641	0.09	43.6	11
11	164	0.40	17.9	44
12	1069	0.20	16.9	46
13	1026	0.86	40.7	72
14	1149	0.79	59.3	89
15	1581	0.63	61.1	88
16a	195	0.20	9.5	30
16b	158	0.53	31.8	86
17	42	0.40	11.7	46
18	32	0.36	7.4	22
19a	233	0.16	14.3	45
19b	14	0.09	82.5	81
20	56	0.56	4.9	15
21	103	0.37	6.8	23
22	77	0.26	8.6	18
23	44	0.10	10.4	12
24	44	NO DATA	4.7	24
25	42	0.12	9.8	33
26	20	0.12	6.9	11
27	38	0.13	8.4	18
28	32	0.10	7.7	15
29	1520	0.62	24.4	74
30	339	0.60	6.8	49
31	750	0.61	27.1	71
32	176	0.29	6.7	49

33	830	0.53	27.1	88
34	461	0.24	17.6	75
35	1429	0.18	55.3	76
36	1818	0.36	10.3	37
37	181	0.48	54.2	94
38	566	0.21	4.5	11
39	303	0.60	7.4	31
40	1660	0.40	18.3	62
41	343	0.25	20.3	56
42	1751	NO DATA	26.8	86

Table B.2. Biological properties of stations sampled as part of the C3O project, but not referenced in this thesis.

C3O Station Name	Net Primary Production (mg C m^{-3} d^{-1})	f-ratio	Total Biomass (mg chl a m^{-3})	Biomass >5 μm (%)
UN-7	19.472	0.36	1.44	7.4
UN-4	19.239	0.56	1.24	24.1
UN-2	19.658	0.55	0.78	57.5
BS-1	48.964	NO DATA	1.42	8.1
BS-3	43.179	NO DATA	1.07	11.7
BCL-6	7.939	0.57	0.14	60.2
BC-4	10.624	0.07	0.31	37.9
BFB-6	0.574	NO DATA	0.06	31.6
BL-4	0	0.44	0.13	19.8
BL-1	10.346	0.10	0.17	24.3
CB28aa	218.067	0.10	0.36	41.8
MK-1	8.371	0.17	0.24	34.7
MK-3	8.904	0.14	0.15	11.7
BE-2	7.170	0.95	0.31	60.3

APPENDIX C. DISSOLVED NUTRIENT CONCENTRATION DATA

Table C.1. Chemical properties (integrated) of stations sampled as part of this thesis. Note that stations 16a and 16b are labelled in the opposite order to those stations in Wyatt (2010).

Station Number	Nitrate (mmol m^{-2})	Ammonium (mmol m^{-2})	Urea (mmol m^{-2})	Silicic Acid (mmol m^{-2})
1	1125.68	NO DATA	26.92	1792.01
2	1210.62	15.58	10.63	996.59
3	741.66	40.79	NO DATA	813.16
4	2112.91	13.60	8.24	2982.34
5	1531.09	22.51	9.49	1445.09
6	1934.10	44.66	19.55	3404.45
7	484.94	77.01	9.35	1690.15
8	1078.77	111.83	31.26	3482.23
9	NO DATA	249.16	54.84	NO DATA
10	362.85	50.04	35.84	1399.76
11	567.60	79.26	21.15	2447.99
12	501.80	150.92	32.51	998.17
13	323.27	31.40	32.24	1172.24
14	173.69	23.28	7.05	700.88
15	408.14	63.57	13.99	1085.80
16a	19.72	9.11	23.06	370.20
16b	252.13	6.21	21.70	834.04
17	549.55	18.30	36.08	1250.14
18	355.86	6.40	11.76	853.98
19a	344.40	5.18	29.03	1535.28
19b	226.38	3.00	13.88	334.25
20	353.89	4.75	47.03	1157.86
21	173.19	4.95	40.04	1013.51
22	293.76	5.30	60.83	870.19
23	770.30	7.95	32.03	2559.29
24	217.91	4.00	24.83	517.59
25	225.95	3.50	21.59	467.00
26	206.69	3.95	52.50	747.18
27	683.52	6.85	45.57	3110.19
28	693.07	4.60	25.39	938.59
29	224.23	3.02	55.90	742.24
30	96.64	5.04	8.75	259.39
31	349.83	5.53	15.76	744.91
32	436.36	17.41	54.31	1015.77

33	278.93	6.76	12.08	417.88
34	131.06	3.26	20.67	243.95
35	140.09	28.39	26.44	491.48
36	393.34	18.94	14.82	628.86
37	123.05	10.00	18.04	169.87
38	427.62	10.01	13.95	555.83
39	518.73	105.64	14.64	130.49
40	216.26	9.07	11.84	222.25
41	352.77	92.15	40.90	169.31
42	289.12	2.99	29.67	313.49

Table C.2. Regional means of dissolved nutrients (Regional Means ± Standard Error).

Region	Dissolved Nitrate (mmol m^{-2})	Dissolved Ammonium (mmol m^{-2})	Dissolved Urea (mmol m^{-2})	Dissolved Silicic Acid (mmol m^{-2})
Northeast Pacific Ocean	1506.1±247.4	27.4±6.4.	12.0±2.6	1928.3±530.8
Bering and Chukchi Seas	394.9±69.1	69.7±22.7	21.4±5.0	1281.0±302.4
South Beaufort Sea	306.2±86.3	9.0±2.4	27.9±6.1	893.2±154.3
Canada Basin	408.1±91.3	5.1±0.5	37.8±9.0	1277.9±350.2
Canadian Arctic Archipelago	261.0±40.6	6.2±1.7	26.3±6.6	661.7±158.4
Baffin Bay and Davis Strait	303.2±67.5	30.3±15.4	16.6±2.1	366.5±88.6

Table C.3. Chemical properties of stations sampled as part of the C3O project, but not referenced in this thesis.

Station Name	Nitrate (μmol L^{-1})	Ammonium (μmol L^{-1})	Urea (μmol L^{-1})	Silicic Acid (μmol L^{-1})
UN-7	1.776	0.431	0.205	15.256
UN-4	0.838	0.168	0.138	15.344
UN-2	0.771	0.179	0.143	8.121
BS-1	3.517	0.532	NO DATA	17.734
BS-3	5.272	1.113	NO DATA	21.948
BCL-6	0.817	0.050	0.227	5.951
BC-4	0.752	0.435	0.386	7.812
BFB-6	0.741	0.050	NO DATA	5.840
BL-4	0.050	0.050	0.202	4.076
BL-1	0.081	0.050	0.924	4.996
CB28aa	0.050	0.050	0.470	4.906
MK-1	0.056	0.050	0.224	11.355
MK-3	0.083	0.050	0.509	12.866
BE-2	9.242	0.128	0.365	16.271